

## Low-temperature adsorption of gases on metal surfaces (Review)

Yu. G. Ptushinskiĭ

Citation: *Low Temp. Phys.* **30**, 1 (2004); doi: 10.1063/1.1645151

View online: <http://dx.doi.org/10.1063/1.1645151>

View Table of Contents: <http://ltp.aip.org/resource/1/LTPHEG/v30/i1>

Published by the [AIP Publishing LLC](#).

---

### Additional information on *Low Temp. Phys.*

Journal Homepage: <http://ltp.aip.org/>

Journal Information: [http://ltp.aip.org/about/about\\_the\\_journal](http://ltp.aip.org/about/about_the_journal)

Top downloads: [http://ltp.aip.org/features/most\\_downloaded](http://ltp.aip.org/features/most_downloaded)

Information for Authors: <http://ltp.aip.org/authors>

## ADVERTISEMENT



**MATERIAL SCIENCE RESEARCH  
AT 3K MADE SIMPLE**

MONTANA INSTRUMENTS  
COLD SCIENCE MADE SIMPLE

CRYOSTATION  
MONTANA INSTRUMENTS

The advertisement features a dark, industrial-themed background with various scientific instruments. On the right, a large black cryostat is prominently displayed with a blue vertical element. In the foreground, a laptop shows a graph with a blue curve. The text is overlaid in white and blue, with the Montana Instruments logo at the bottom center.

## LOW-TEMPERATURE MAGNETISM

---

### Low-temperature adsorption of gases on metal surfaces (Review)

Yu. G. Ptushinskii\*

*Institute of Physics of the National Academy of Sciences of Ukraine, pr. Nauki 46, Kiev 03028, Ukraine*  
(Submitted April 29, 2003)

Fiz. Nizk. Temp. **30**, 3–37 (January 2004)

A review of the published results on the adsorption of some simple gases on metal surfaces at low substrate temperatures ( $T_s \leq 30$  K, down to liquid helium temperatures) is given.

The methods of investigating low-temperature adsorption of gases are briefly discussed. Attention is focused primarily on the adsorption of hydrogen on transition metals and noble metals.

The results of experimental studies on transition metals include information about the state of the adsorbed particles (atoms or molecules), the spectra of the adsorption states, the kinetics of adsorption–desorption processes, the participation of precursor states in the adsorption mechanism, the role of various quantum properties of the  $H_2$  and  $D_2$  molecules, the influence of two-dimensional phase transitions, the structure of the adsorbed layer (adlayer), and electron-stimulated processes. Experimental studies of the adsorption of hydrogen on noble metals in conjunction with theoretical calculations provide information about the fine details of the quantum sticking mechanism, in particular, the trapping of molecules into quasi-bound states and the influence of diffraction by the lattice of surface atoms. Data on the role of the rotational state of the molecules, ortho–para conversion, and direct photodesorption are examined.

A review of the relatively few papers on the adsorption of oxygen, carbon monoxide, and nitrogen is also given. © 2004 American Institute of Physics. [DOI: 10.1063/1.1645151]

## INTRODUCTION

### 1.1. Gas adsorption and its role

The key role of adsorption in a number of important processes in technology and in the living world is widely known. It suffices to mention heterogeneous catalysis, micro- and nanoelectronics, hydrogen fuel storage, hydrogen embrittlement of metals, corrosion, and the assimilation of atmospheric nitrogen by living organisms. Adlayer are, among other things, low-dimensional systems, and the study of their properties is extremely important for basic physics.

For these reasons there is enormous interest in the study of adsorption processes, and a huge number of both experimental and theoretical papers have been published. The assimilation of ultrahigh-vacuum technique into experimental physics in the early 1960s and the development of many extremely informative surface diagnostic techniques have made for unprecedented progress in this field. As examples we can name the methods of temperature-programmed desorption (TPD) or thermodesorption spectroscopy (TDS), low-energy electron diffraction (LEED), Auger electron spectroscopy (AES), ultraviolet and x-ray photoelectron spectroscopy (UPS and XPS), electron energy-loss spectroscopy (EELS) and its high-resolution version (HREELS), scanning tunneling microscopy (STM), etc.

It would be impossible (and hardly necessary) to cover all of this immense field in a single review article. We have therefore drastically narrowed the scope: First, we consider only adsorption systems in which the adsorbents (substrates) are metals and the adsorbates are molecules of simple gases.

Second, we concentrate mainly on low-temperature adsorption, arbitrarily taking  $T_s = 30$  K as the boundary of the adsorbent temperature region considered.

There are several features that make low-temperature adsorption particularly interesting. At sufficiently low temperatures it is possible for weakly bound, physisorbed molecules to be held on the surface and investigated experimentally. Molecular adsorption states are often encountered in the role of precursor states for dissociative chemisorption. Thus the study of the behavior of molecules in such states is important for understanding the mechanism of dissociative adsorption, which is the key stage in the processes mentioned above. The initial stage is the adsorption of monolayers of molecules at low temperatures, which is also of interest for studying the growth of cryocrystals. Studies of the phase state of physisorbed quasi-two-dimensional layers and of possible isotope effects (especially topical in the case of hydrogen) also require experiments at low substrate temperatures and are of independent interest.

As we have said, there have been an enormous number of papers devoted to the study of adsorption, and their results have been summarized in a number of reviews and monographs (see, e.g., Refs. 1–6). However, this is not the case for low-temperature adsorption. We know of only the review by Ilisca<sup>7</sup> in 1992, devoted to ortho–para conversion of physisorbed hydrogen molecules, and the recently published review by Panchenko *et al.*<sup>8</sup> of research on galvanomagnetic size effects on metal surfaces and the use of these effects to study adsorption and processes of ordering of the adsorbate layer. A cursory discussion of the problem of low-

temperature adsorption of gases is given in the review by Naumovets.<sup>9</sup> It should be mentioned that the number of original papers on low-temperature adsorption of gases also falls far short of the number of papers on the adsorption of gases under ordinary temperature conditions. It is our intention to fill this gap in some measure and to discuss research results on the low-temperature adsorption of gases without restriction to a particular technique or surface-sensitive effect.

## 1.2. General qualitative ideas about the mechanism of gas adsorption on metals

Although molecular physisorption is peculiar to low substrate temperatures, dissociative chemisorption also occurs under these conditions, as will be seen below. It is therefore advisable to touch upon the mechanism of dissociative adsorption of molecular gases. The current ideas as to the mechanism of dissociative adsorption are based on the results of experimental research using molecular beams (most often supersonic with a small spread of molecular energies<sup>2</sup>) and theoretical quantum-dynamics calculations of the multi-dimensional potential energy surface,<sup>1,5,10</sup> though mainly for hydrogen molecules. Of course, the six-dimensional potential energy surface cannot be illustrated, and one often resorts to showing two-dimensional sections through it.<sup>6</sup>

However, for a qualitative interpretation of the experimental results and for greater lucidity, one can even use a one-dimensional Lennard-Jones potential diagram, shown schematically in Fig. 1.<sup>11</sup> As it approaches the surface, a molecule first experiences a van der Waals attraction, which then gives way to Pauli repulsion due to the overlap of the tails of the Bloch wave functions of the metal and the filled

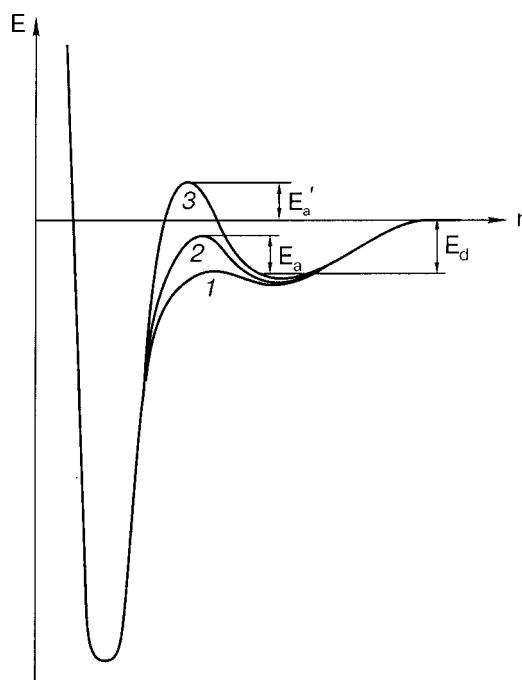


FIG. 1. One-dimensional potential diagram. Chemisorption: 1—direct; 2—via a precursor state; 3—activated.  $E_a$  is the activation energy for the transition from the precursor state to a state of chemisorption,  $E_d$  is the activation energy for desorption, and  $E'_a$  is the activation energy for adsorption.

orbitals of the molecule. These two interactions form a shallow physisorption potential well, which, as the molecule approaches still closer to the surface, gives way to a deep chemisorption well. Between these potential wells is a barrier whose value depends on the mechanism of dissociative adsorption. One can distinguish three types of barrier: 1—The barrier is negligible, and the molecule is not held in a state of physisorption but slides into the chemisorption well. 2—The barrier is appreciable but does not reach the zero level of energy (the potential energy of the molecule at infinite separation). The molecule will spend some time in a state of physisorption and with a certain probability will either pass to a state of chemisorption or be desorbed. This is the mechanism of chemisorption with the participation of a precursor state. Two types of precursor states are distinguished: above an unoccupied adsorption center (intrinsic) and above an occupied center (extrinsic).<sup>12</sup> 3—The barrier is higher than the zero level of energy. For passage to a state of chemisorption a kinetic energy sufficient to overcome this potential barrier must be imparted to the molecule. This is the mechanism of activated chemisorption.

Harris and Andersson<sup>13</sup> considered the transformation of the electronic structure of a (hydrogen) molecule and a metal as they approach. The situation is essentially different for a noble metal (copper) and a transition metal (nickel). In both cases the dissociation of the molecule occurs due to the transfer of electrons from the metal to the antibonding  $\sigma_u$  orbital of the  $H_2$  molecule. Since in the case of copper this process involves 4s electrons of the metal, the overlap of their wave functions with the filled  $\sigma_g$  orbital of hydrogen forms an activation barrier, and the aforementioned transfer of electrons to the  $\sigma_u$  orbital can occur only after an activation barrier is overcome. The height of the activation barrier depends on the properties of the interacting partners. For example, according to Ref. 13, for the  $H_2/Na$  system the barrier height is equal to 0.2 eV, while for  $H_2/Al$  it is 1 eV.

A different situation arises in the case of the transition metal nickel. Because of the presence of unfilled  $d$  states near the Fermi level, when a molecule approaches sufficiently close to the surface the  $3d$  levels lie below the  $4s$  levels on the energy scale, and the latter are vacated. This transition of electrons to the compact  $3d$  orbitals prevents the formation of a Pauli activation barrier, and on closer approach to the surface the molecule dissociates.

This qualitative picture of the adsorption interaction of a molecule with a metal surface is not specific for low-temperature adsorption and is suitable for the description of adsorption under any temperature conditions. We will stop at this brief description of the adsorption mechanism and turn to a discussion of the techniques used in the experimental study of low-temperature adsorption of gases.

## 2. METHODS OF STUDY OF LOW-TEMPERATURE ADSORPTION OF GASES

The general requirements for experimental research on gas adsorption (not only at low temperature) are ultrahigh-vacuum conditions (residual gas pressure  $\leq 10^{-10}$  torr) and control of the atomic purity and structure of the surface and of the purity of the gas under study. These are usually monitored by the methods of AES, LEED, and mass spectrometry.

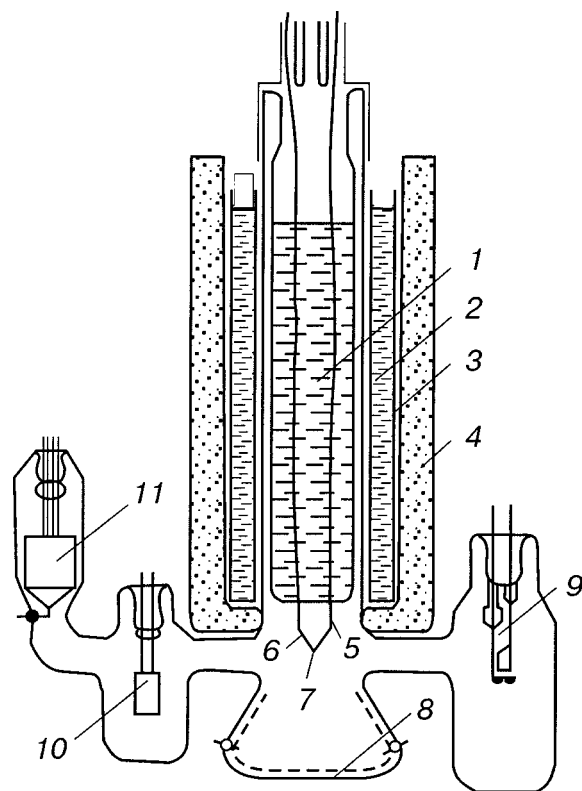


FIG. 2. Field-emission projector with a cooled tip.<sup>17</sup> 1—Dewar foot containing liquid helium; 2—copper vessel; 3—liquid nitrogen; 4—foam plastic thermal insulation; 5—molybdenum leads; 6—tungsten arch; 7—tungsten tip; 8—luminescent screen; 9—titanium pump; 10—hydrogen source; 11—manometer.

Let us briefly discuss some of the techniques used to acquire data on the characteristics of the low-temperature adsorption of gases. Since all of the techniques used for adsorption studies are thoroughly described in the literature, we will only briefly touch on the features of their application in the low-temperature region.

### 2.1. The field-emission microscope (FEM) method<sup>14,15</sup>

The earliest paper known to the author on the use of the FEM method for studying the mobility of hydrogen on the surface of a tungsten tip cooled by liquid helium is that of Gomer *et al.*<sup>16</sup> An adlayer of hydrogen was deposited on a region with a sharp boundary on the surface of the tip, and the advance of this boundary to the uncoated part was tracked. A device of this type has also been used by Medvedev and Snitko in a study of the field emission of hydrogen ions.<sup>17</sup> A diagram of this device is shown in Fig. 2. Later Mazenko, Banavar, and Gomer modified the FEM method for measuring the parameters of surface diffusion by observation of the correlation of the fluctuations of the field emission current from different parts of the tip.<sup>18</sup>

The FEM method was also used by Polizotti and Erlich for a comparative study of the adsorption of hydrogen (and nitrogen) on different faces of tungsten and rhodium, although at tip temperatures not lower than 38 K.<sup>19</sup>

### 2.2. The low-energy electron diffraction (LEED) method

The LEED method is one of the most informative and widely used methods for studying the structure of the surface

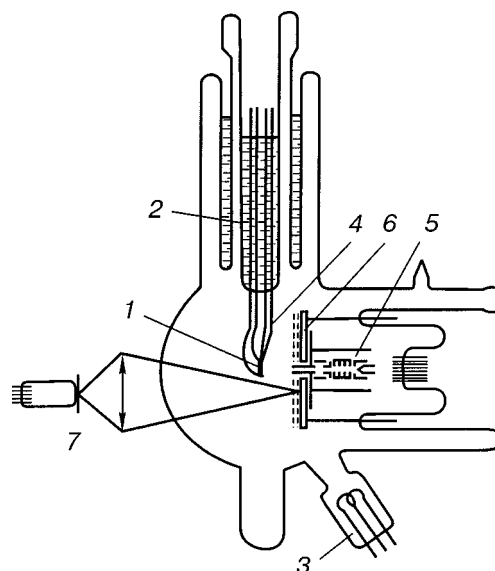


FIG. 3. Glass electronograph with cooled sample.<sup>20</sup> 1—Sample; 2—foot with liquid helium; 3—hydrogen source; 4—thermocouple; 5—electron gun; 6—luminescent screen; 7—telescopic photometer.

and of the adlayer. Figure 3 shows a diagram<sup>20</sup> of a low-voltage electronograph in a glass envelope, created by Fedorus for investigating the structure of adlayers at  $T_s \sim 5$  K. Fedorus also developed an electronograph that can be mounted in a metallic Riber ultrahigh-vacuum unit and is intended for operation at  $T_s \sim 5$  K.<sup>21</sup> An electronograph of a similar type was made by Strongin *et al.*<sup>22</sup>

### 2.3. Method of galvanomagnetic size effect

Panchenko and co-workers have developed a method of studying the low-temperature adsorption of gases based on measurement of the magnetoresistance (static skin effect<sup>23</sup>) and the Sondheimer oscillations<sup>24</sup> in thin single-crystal slabs of a metal (mainly tungsten). Figure 4 shows a diagram<sup>25</sup> of a glass ultrahigh-vacuum device designed for studying the static skin effect and equipped with a low-voltage electronograph.

The method is based on the fact that the scattering and diffraction of conduction electrons on the surface are sensitive to its structure and the structure of the adlayer, and one can therefore assess the structural changes from the variation of the magnetoresistance during the adsorption process. An important feature of the method is its nondestructive character. To become acquainted with the details of this method we recommend the review article cited as Ref. 8.

### 2.4. Methods of electron spectroscopy<sup>26</sup>

Several versions of electron spectroscopy are used to study the low-temperature adsorption of gases: Auger electron, ultraviolet and x-ray photoelectron, and electron energy loss. To determine the physical state and the character of the excitations of gaseous adsorbates at low  $T_s$  a particularly effective method is high-resolution electron energy loss spectroscopy (HREELS).<sup>27,28</sup>

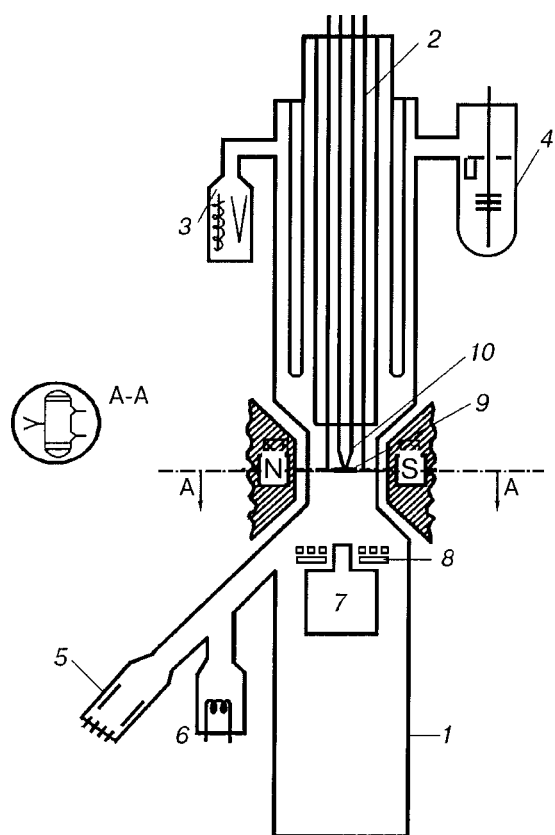


FIG. 4. Device combining the static skin-effect and LEED methods.<sup>8,25</sup> 1—Glass envelope; 2—helium cryostat; 3—manometer; 4—getter pump; 5,6—sources of adsorbate; 7—electron gun; 8—grids and luminescent screen; 9—sample; 10—thermocouple.

## 2.5. Methods of molecular beam and temperature-programmed desorption

To determine such parameters of the low-temperature adsorption as the surface density of molecules  $n$ , the sticking coefficient  $S$ , the spectra of the adsorption states, and the activation energy for desorption, ultrahigh-vacuum equipment is used to implement the molecular-beam and temperature-programmed desorption methods. The molecular-beam method is used in two modifications: with a source of the effusion or supersonic-nozzle<sup>29</sup> type. The latter has the advantage of a lower energy spread of the molecules in the beam, but it is more complicated to implement because of the necessity of several steps of differential pumping.

An extremely refined apparatus with a monoenergetic molecular beam of the nozzle type has been built at Chalmers University and is described in Ref. 30. The apparatus has been used to study the sticking (and scattering) of normal gases ( $n\text{-H}_2$  and  $n\text{-D}_2$ ) and also of the para and ortho modifications ( $p\text{-H}_2$  and  $o\text{-D}_2$ ) with the goal of elucidating how the sticking is influenced by the rotational states of the molecules. The beams of the latter molecules were obtained by conversion of the normal gases with the use of a nickel silicate catalyst at a temperature of 25 K. A single-crystal copper sample was cooled by helium gas to  $T_s \sim 10$  K. The detector of the scattered molecules was a movable ionization manometer with a narrow entrance channel, making it possible to observe the diffraction of the molecular beam on the surface of the sample. The apparatus had provisions for vary-

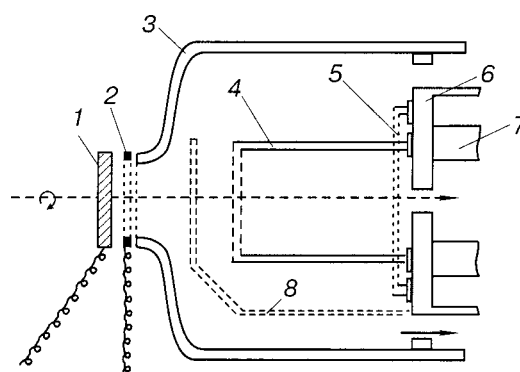


FIG. 5. Fragment of the restricted-volume apparatus for accumulation of the desorbed gas.<sup>31</sup> 1—Sample; 2—capacitive ring; 3—glass bell jar; 4—ion source chamber; 5—filament of the ion source; 6,7—parts of the quadrupole mass spectrometer; 8—baffle.

ing the angle of incidence of the molecular beam over rather wide limits. Measurement of the sticking coefficient as a function of coverage was done by recording the partial pressure of the gas under study in the main chamber with the aid of a mass spectrometer during both the gas adsorption and desorption processes.

An extremely original method of measuring the sticking coefficient and coverage was implemented by Schlichting and Menzel.<sup>31</sup> Those parameters were determined from the increase in pressure during the thermodesorption of adsorbed particles in a glass bell jar of small volume in which the ion source of the mass spectrometer was placed. The bell jar was separated from the main chamber by a narrow gap with low transmission. This measure improves the sensitivity of the thermodesorption method considerably in comparison with that obtained when the pressure increase is registered in the main chamber of large volume. After completion of an adsorption cycle the liquid-helium-cooled sample is moved into position in front of the entrance of the bell jar and the thermodesorption is carried out. This part of the experimental apparatus is shown schematically in Fig. 5.<sup>31</sup> The gas under study was delivered to the sample from an effusion source. The cooling of the sample was done through a copper block in contact with the liquid helium.<sup>32</sup>

Finally, let us briefly discuss the technique used in the author's laboratory for studying low-temperature adsorption of gases. We have built an ultrahigh-vacuum device of the "black chamber" type,<sup>33,34</sup> the basic features of which are the possibility of forming an effusion molecular beam and the line-of-sight registration of the desorbed or scattered molecules. The line-of-sight registration regime eliminates the influence of secondary processes on the chamber walls, which distorts the results of the measurements. The line-of-sight registration regime and the formation of the molecular beam were achieved by means of a double-walled jacket built into the vacuum chamber; the jacket was cooled by liquid nitrogen and was coated with a freshly deposited titanium film. This apparatus is shown schematically in Fig. 6.<sup>34</sup> The cooling of the sample was done through a copper rod directly in contact with liquid helium poured into the tubular manipulator. A tungsten tube was tightly fitted on the rod, and the sample was resistance welded to the opposite end of the tube to form a bottom.

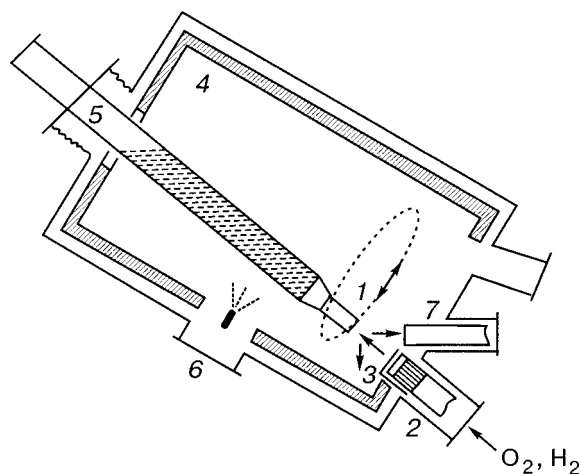


FIG. 6. Diagram of an apparatus with an effusion molecular beam and line-of-site registration.<sup>34</sup> 1—Sample; 2—source of molecular beam; 3—baffle; 4—nitrogen-cooled jacket; 5—manipulator; 6—titanium evaporator; 7—mass-spectrometric detector.

Let us discuss the definitions of such parameters of the adsorption process as the sticking coefficient (or sticking probability)  $S$  of a molecule, the surface density  $n$  of the adsorbate (or the degree of coverage  $\theta$ ), and the spectrum of the adsorption states. The sticking coefficient is the fraction of molecules that stick from the flow incident on the surface:

$$S = \frac{dn}{dt} \frac{1}{F}, \quad (2.1)$$

where  $F$  is the flux density of molecules onto the surface.

There are two main methods of measuring the sticking coefficient. One of them is to differentiate the experimental time dependence of the surface density determined by the thermodesorption method. This method was used, e.g., by Friess, Schlichting, and Menzel.<sup>35,36</sup> The second method is based on measurement of the flux density of molecules scattered or desorbed by the surface. We shall mention two variants of this method. The first was proposed by King and Wells<sup>37,38</sup> and is based on measurement of the gas pressure in the chamber under conditions when the molecular beam is incident on the surface of the sample and when the sample has been moved to the side of the molecular beam zone. The second variant was proposed by Bosov and Chuikov<sup>39</sup> and is based on continuous measurement of the flux density of scattered or desorbed molecules through the ion source of a mass-spectrometric detector prior to interaction with the walls of the chamber. The importance of the latter condition, especially in measurement of the thermodesorption spectrum, is illustrated by the results of Refs. 40 and 41. The oxygen thermodesorption spectrum measured under conditions when the desorbed particles can strike the ion source not only directly but also after interacting with the walls contains CO, O<sub>2</sub>, and CO<sub>2</sub> as well as atomic oxygen.<sup>40</sup> However, if the influence of the walls is eliminated, then only atomic oxygen remains in the spectrum.<sup>41</sup>

In the method of Bosov and Chuikov the sticking coefficient is determined from the equation

$$S(t) = 1 - I(t)/I_m, \quad (2.2)$$

where  $I(t)$  and  $I_m$  are the ion currents of the detector at time  $t$  and after the formation of a saturated adlayer, respectively. The surface density of molecules is determined from the equation

$$n(t) = F \int_0^t S(t) dt. \quad (2.3)$$

The degree of coverage  $\theta(t) = n(t)/n_a$ , where  $n_a$  is the density of surface atoms of the substrate ( $\sim 1.4 \times 10^{15}$  for the (110) face of W and Mo). If this is not specifically stipulated, we shall henceforth use  $\theta$  to mean to number of molecules per surface atom of the substrate, regardless of whether or not the molecule is dissociated.

Let us turn to a discussion of the research results on the low-temperature adsorption of gases. We shall concentrate in the greatest detail on the results for hydrogen, in less detail on the results for oxygen, and only briefly on those for carbon monoxide and nitrogen, primarily because of the volume of published results for these gases but also to reflect the scientific interests of the author. For brevity we use the following terms used in the literature: *adatom* for adsorbed atom, *admolecule* for adsorbed molecule, *adparticle* for adsorbed particle, and *adlayer* for adsorbed layer.

### 3. HYDROGEN

Hydrogen is the simplest of the simple gases (H<sub>2</sub>, N<sub>2</sub>, O<sub>2</sub>, CO, CO<sub>2</sub>). The hydrogen atom has only one electron (the molecule, two), and that makes it amenable to theoretical treatment of the adsorption interaction with a metal surface. Hydrogen is of considerable interest from the standpoint of practical use, as a participant in important catalytic processes (e.g., the synthesis of ammonia), as a prospective environmentally clean fuel, etc. The key link in catalysis and in the dissolution of hydrogen fuel in a solid-state carrier is the dissociative chemisorption of hydrogen. Hydrogen isotopes have a unique mass ratio (D<sub>2</sub> is twice as heavy as H<sub>2</sub>), making it the most favorable for manifestation of various isotope effects.

The study of hydrogen adsorption at low temperatures is of both purely scientific and applied interest. It is only for temperatures close to liquid-helium temperature that hydrogen can be steadily held in molecular adsorption states on a surface and that one can study the properties of such physisorbed layers, including phase transitions, isotope effects, and quantum effects in them. In addition, physisorbed molecules can act as precursor states for dissociative chemisorption, and the study of the behavior of molecules in a state of physisorption is very important for understanding the mechanism of chemisorption.

#### 3.1. Adsorption-desorption processes for hydrogen on the surface of transition metals

##### 3.1.1. Dissociative chemisorption

An important characteristic of an adsorption system is the state of the adsorbed particles: dissociative atomic or molecular. In particular, only those surfaces on which dissociative chemisorption occurs can be catalytically active. The first papers known to the author on the low-temperature ( $T_s \sim 4.2$  K) adsorption of hydrogen on tungsten were published in 1955–1957 by Gomer *et al.*<sup>16,42,43</sup> A detailed de-

scription of the experiments and results is given in Ref. 16. The experiments were done in a field-emission projector with a tungsten tip cooled by liquid helium. A hydrogen adlayer with a sharp boundary was deposited on one side of the tip, and the propagation of the boundary along the (110) surface at the end of the tip was followed on a luminescent screen. At high coverages the motion of the boundary was observed even at  $T_s < 20$  K and was attributed to the migration of physisorbed hydrogen molecules along a chemisorbed atomic layer. If the initial coverage was substantially lower, the motion of the boundary began only at  $T_s \geq 180$  K, and this was most likely surface diffusion of atomic hydrogen. Thus the authors of Ref. 16 arrived at the conclusion that dissociative chemisorption of hydrogen on the clean W(110) surface occurs at liquid-helium temperature.

Polizotti and Erlich<sup>19</sup> arrived at the opposite conclusion. Studying hydrogen adsorption at  $T_s = 80$  K in a field-emission projector, they observed<sup>19</sup> that the change in the (electron) work function  $\varphi_{110}$  of the W(110) face (measured using a probe orifice) begins only after the averaged work function over the whole tip,  $\varphi_{\text{mean}}$ , has stopped changing. Since the change in work function is caused by adsorption, those authors<sup>19</sup> concluded that dissociative adsorption of hydrogen on W(110) does not occur under those conditions, and the delayed change in  $\varphi_{110}$  is due to the creeping of hydrogen atoms from the peripheral less densely packed parts of the tip. At  $T_s = 38$  K the work functions  $\varphi_{110}$  and  $\varphi_{\text{mean}}$  vary synchronously, but when the tip is heated to 77 K,  $\varphi_{110}$  returns to its original value with no sign of conversion of molecular to atomic hydrogen. Thus the authors of Ref. 19 assert that dissociative adsorption of hydrogen does not occur on the W(110) surface at low temperature.

It is hard to assess the reasons for such a difference in the conclusions of Refs. 16 and 19. One can only assume that the character of the change in work function measured from the field-emission current from a very small part of the surface is affected by the high electric field necessary for field emission. Although a high field was also present in the experiments of Ref. 16, the characteristic of the adsorption was not judged from the work function but from the motion of the boundary of the adlayer on the field-emission image. Below we give several more arguments in favor of dissociative adsorption at  $T_s \sim 5$  K, based on experiments with macrocrystals in the absence of any electric field.

The thermodesorption spectrum (Fig. 7)<sup>44</sup> of the hydrogen adlayer formed on the W(110) surface at  $T_s \sim 5$  K, in addition to having the low-temperature peaks belonging to molecular adsorption states (the details of which are discussed below), also contains two high-temperature peaks (410 and 550 K), which belong to atomic chemisorption and have been observed previously by Tamm and Schmidt.<sup>45</sup> The atomic nature of these states has been established by the isotopic exchange method.<sup>45,46</sup> Granted, it cannot in principle be ruled out that the atomic chemisorbed phase was formed not in the process of adsorption at 5 K but as a result of conversion of the molecular phase at a higher temperature. However, the results of Ref. 46 prove that that is not the case. If the molecular phase of the adsorption participated in the formation of the atomic phase, then the number of molecules in the low-temperature phase of desorption would be

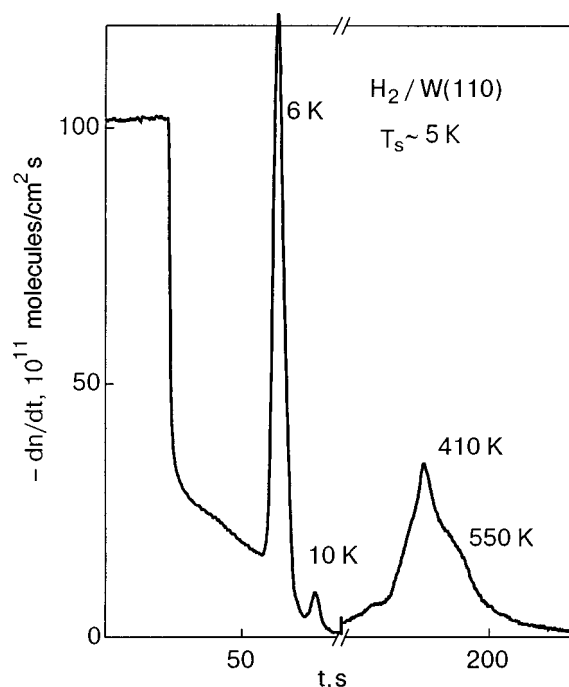


FIG. 7. Thermodesorption spectrum for hydrogen.<sup>44</sup>

substantially smaller in the case when the adsorption occurs on the initially clean surface than in the case of adsorption on a previously formed atomic phase (in the latter case the molecular phase would not be expended on the formation of the atomic phase). In actuality, the thermodesorption spectra in the two cases were found to be identical.

More evidence for dissociative adsorption of hydrogen on W(110) at  $T_s \sim 5$  K in the initial stage of the process is given by the character of the dependence of the sticking coefficient on the degree of coverage,  $S(\theta)$ . The accumulation of weakly bound molecules on the surface from the very start of the adsorption process should be accompanied by an increase in the sticking coefficient, as was observed by Andersson *et al.*<sup>30</sup> for the adsorption of  $H_2$  on copper, when dissociation of the  $H_2$  molecules does not occur. The results of experiments on the  $H_2/W(110)$  system attest to a decrease in the sticking coefficient with increasing coverage in the initial stage. This is seen in Fig. 8, taken from Ref. 47 (for more details about  $S(\theta)$  see below).

Evidence for a dissociative mechanism of hydrogen adsorption on the W(111) surface at  $T_s \sim 5$  K is given by the results of Refs. 46 and 48. This evidence comes from the isotopic exchange for the high-temperature peaks of the desorption and the absence of an influence of the substrate temperature on the kinetics of the initial stage of adsorption in the interval 5–150 K. If a change in the adsorption mechanism occurred in going from  $T_s = 150$  K to  $T_s = 5$  K, this would be reflected in the kinetics of the process. The statement that the adsorption of hydrogen (and deuterium) on the transition metal ruthenium at  $T_s \sim 5$  K is of a dissociative character in the initial stage of the process was made in the paper by Friess, Schlichting, and Menzel.<sup>35</sup> Indirect signs of dissociative adsorption of hydrogen on Mo(110) at  $T_s \sim 5$  K can be found in Ref. 49, which will be discussed in more detail below.

Thus there are sufficient grounds, in my view, to assert

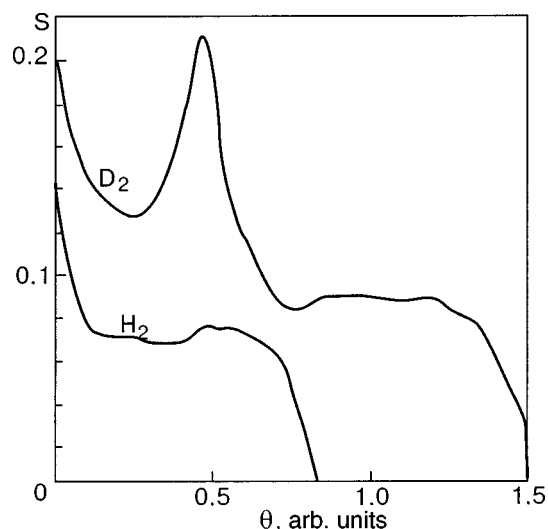


FIG. 8. Sticking coefficient for  $H_2$  and  $D_2$  versus the degree of coverage.<sup>47</sup>

that dissociative chemisorption of hydrogen (deuterium) occurs at  $T_s \sim 5$  K on the surface of transition metals (W, Mo, Ru) in the initial stage of the process up until the formation of a monoatomic layer, after which molecular adsorption phases are formed on the metal surface coated by the chemisorbed monolayer of atoms.

**3.1.1.1. Initial sticking coefficient.** Information about the initial sticking coefficient  $S_0$  (for  $\theta \rightarrow 0$ ) and the influence on it of such factors as the substrate temperature and the temperature and pressure (flux density) of the gas being adsorbed are of significant interest as a source of information about the character of the gas-metal interaction potential, in particular, about the question of which of the versions of the potential in Fig. 1 is realized. Since in the initial stage the adsorption of  $H_2$  on transition metals at low temperatures is dissociative, it is appropriate to examine the data on the initial sticking coefficient in the Section devoted to dissociative adsorption. Figures 9 and 10 show the dependence of the initial sticking coefficient on the gas temperature,  $S_0(T_g)$ ,

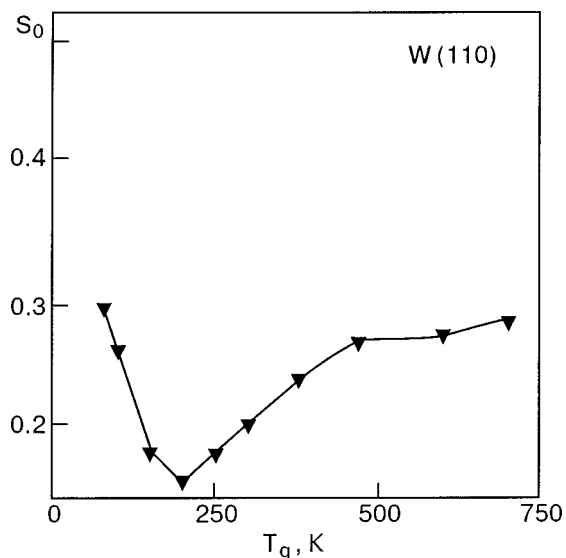


FIG. 9. Initial sticking coefficient for  $D_2$  on W(110) versus the gas temperature.<sup>47</sup>

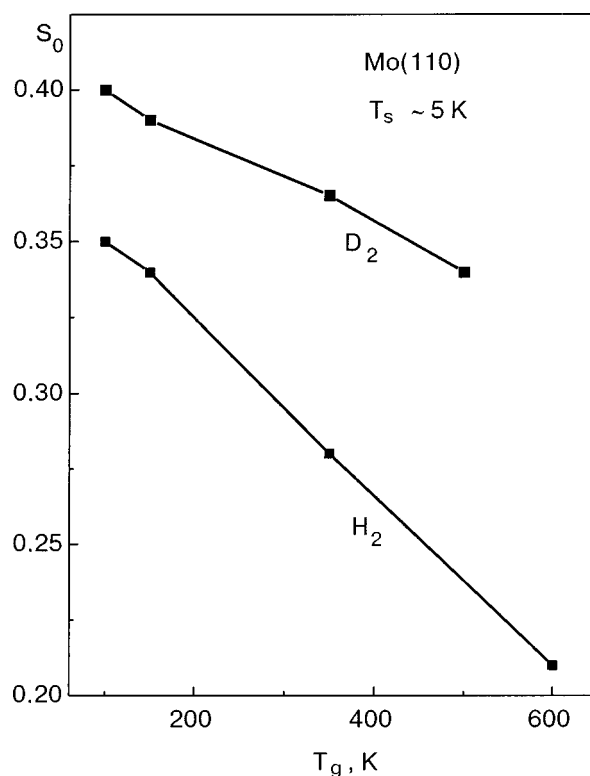


FIG. 10. Initial sticking coefficient for  $H_2$  and  $D_2$  on Mo(110) versus the gas temperature.<sup>49</sup>

for the systems  $D_2/W(110)$  (Ref. 47) and  $H_2/Mo(110)$  and  $D_2/Mo(110)$  (Ref. 49), respectively. In the case of  $D_2/W(110)$  the dependence is nonmonotonic:  $S_0$  decreases with increasing  $T_g$  for  $T_g < 200$  K and increases for  $T_g > 200$  K. This sort of dependence of  $S_0(T_g)$  for the adsorption of  $D_2$  on W(110) attests to the presence of two channels of adsorption: 1) via an intrinsic precursor state, in which case the probability of capture to the precursor state naturally decreases with increasing kinetic energy of the incident molecule; 2) through an activation barrier, when the probability of dissociative chemisorption by overcoming of the barrier increases with increasing kinetic energy of the molecules. Thus two versions of the potential, 2 and 3 in Fig. 1, are operative in this case.

In the case of adsorption on Mo(110), both for hydrogen and for deuterium, a monotonic decrease of  $S_0$  with increasing  $T_g$  is observed (Fig. 10), i.e., dissociative adsorption occurs predominantly by the second path—via an intrinsic precursor state. It should be noted that this last assertion is not indisputable, and some authors give preference to a steering-effect mechanism, which also explains the decrease of  $S_0$  with increasing  $T_g$  (Refs. 50–54). The essence of the steering effect is that a molecule coming in slowly has more time to come to the energetically most favorable configuration in the field of the surface forces. Although this effect is quite possible, and there is experimental evidence of its important role,<sup>52–54</sup> the participation of a precursor state in the mechanism of dissociative adsorption of hydrogen cannot be disregarded in the calculations. In particular, the results of Ref. 55, discussed below, are evidence of this.

Figure 11, taken from Ref. 55, shows the dependence of  $S_0$  on the flux density of  $H_2$  and  $D_2$  molecules on W(110). In



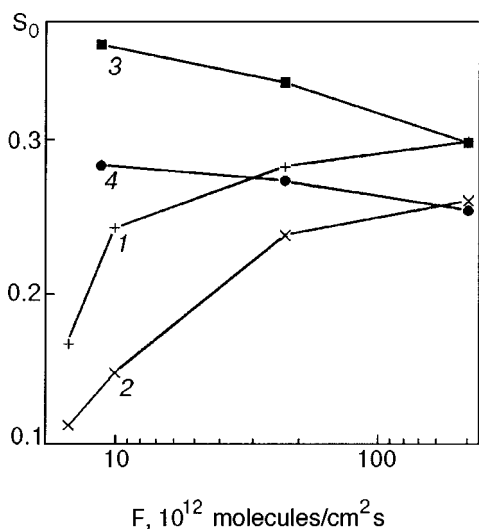


FIG. 11. Initial sticking coefficient for  $H_2$  and  $D_2$  on W(110) versus the flux density of gas molecules.<sup>55</sup> 1,3—For  $H_2$  and  $D_2$ , respectively, on the clean surface; 2,4—for  $H_2$  and  $D_2$  on a surface coated beforehand with a chemisorbed monolayer.

the case of  $H_2$  an appreciable growth of  $S_0$  is observed as the flux density increases from  $\sim 5 \times 10^{12}$  to  $2 \times 10^{14}$  molecules/cm<sup>2</sup>s. There appears to be no doubt that the observed variation of  $S_0$  with increasing  $S_0$  can occur in the case when the adsorption mechanism involves the participation of an intrinsic precursor state, and the molecules sojourning in the precursor state interact with each other. It is shown in Ref. 55 that when the data on the mobility of  $H_2$  molecules in the precursor state and the real characteristics of the instrumentation are taken into account, the approach and interaction of molecules in the precursor state are entirely possible, and the increase in the sticking coefficient is due to the formation of clusters of a 2D condensed phase and the hindered thermodesorption of molecules from such clusters. If the elastic reflection of molecules is ignored, the sticking coefficient can be expressed as follows:<sup>11,56</sup>

$$S_0 = \left[ 1 + \frac{\nu_d}{\nu_a} \exp\left(\frac{E_a - E_d}{kT_s}\right) \right]^{-1}, \quad (3.1)$$

where  $\nu_a$  and  $\nu_d$  are frequency factors,  $E_a$  and  $E_d$  are the activation energies for the transition from the precursor state to a state of chemisorption and desorption, respectively. The activation energy for desorption of a molecule from a cluster should be larger because of the lateral attractive interaction of the molecules in the cluster. It is seen from Eq. (3.1) that an increase of  $E_d$  leads to an increase of  $S_0$ .

As is seen in Fig. 11, for deuterium adsorption such an increase of  $S_0$  with increasing flux density does not occur (moreover,  $S_0$  even exhibits a slight decrease which has not yet been explained). We assume that the absence of an increase in  $S_0$  for deuterium is the impossibility of forming clusters of a 2D phase as in the case of hydrogen. This, in turn, is explained by the deeper position of the level of zero-point vibrations of the  $D_2$  molecule in the physisorption potential well, i.e., the deeper potential relief along the surface than in the case of  $H_2$ . The influence of quantum tunneling diffusion in the case of hydrogen also cannot be ruled out. There is no other apparent explanation for the growth of the

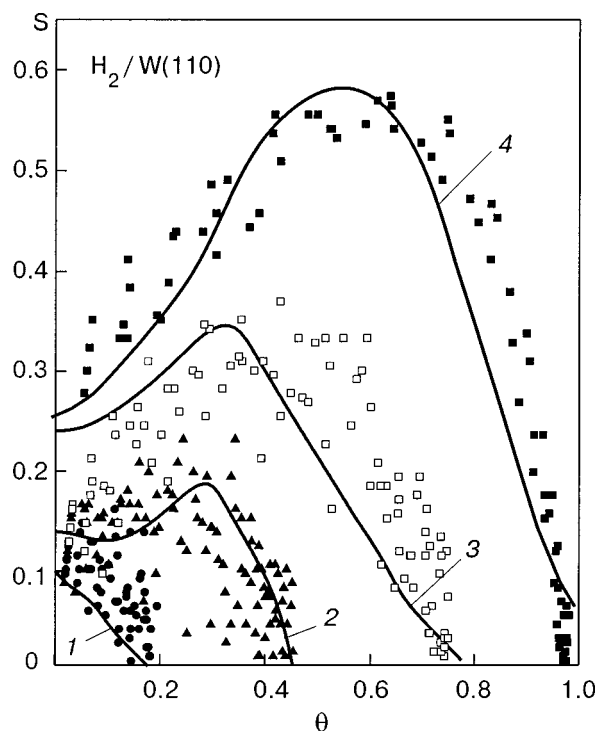


FIG. 12. Sticking coefficient versus degree of coverage for  $H_2$  on the W(110) surface filled beforehand with a chemisorbed monolayer.<sup>59</sup> The solid curves are experimental, the points are from a Monte Carlo simulation; flux density  $F$  [ $\text{cm}^{-2}\text{s}^{-1}$ ]:  $0.6 \times 10^{13}$  (1),  $0.9 \times 10^{13}$  (2);  $4 \times 10^{13}$  (3);  $20 \times 10^{13}$  (4).

initial sticking coefficient with increasing flux density at  $T_s \sim 5$  K on W(110) except an interaction of the molecules in the intrinsic precursor states and, thus, at least for the  $H_2$ /W(110) system, such an interaction is operative.

### 3.1.2. Adsorption–desorption processes in the molecular phase

**3.1.2.1. Adsorption kinetics.** To the author's knowledge the kinetics of low-temperature adsorption of hydrogen on transition metals has been investigated in our previous studies for W and Mo (Refs. 46–49, 55, 57, and 58) and by Friess, Schlichting, and Menzel for ruthenium.<sup>35</sup>

Figure 12, taken from Ref. 59, shows the dependence of the sticking coefficient for  $H_2$  on the coverage for a W(110) surface filled beforehand by a chemisorbed monolayer of hydrogen atoms. Such a surface was formed by annealing at  $\sim 100$  K a sample previously saturated with hydrogen at  $T_s \sim 5$  K. The  $S(\theta)$  curves were obtained at different intensities of the molecular beam. The solid curves show the experimental dependence<sup>55</sup> and the points show the results of a Monte Carlo computer simulation.<sup>59</sup> Let us first discuss one of the curves, e.g., that for the highest flux density,  $F = 2 \times 10^{14}$  molecules/cm<sup>2</sup>s. The observed growth of the sticking coefficient with coverage is explained by an increase in the efficiency of kinetic energy loss by the incident molecule in its collision with a previously adsorbed, weakly bound molecule. This occurs because the masses of the collision partners become equal, whereas when striking the clean surface or a surface coated with tightly bound hydrogen atoms the mass difference is very large and the accommodation coefficient

cient is small. A similar growth of the sticking coefficient with increasing coverage in a molecular adsorbed phase was observed in our earlier studies<sup>47,58</sup> for W(110) and also by Friess, Schlichting, and Menzel for ruthenium,<sup>35</sup> and by Andersson *et al.*<sup>30</sup> and by Wilzen *et al.*<sup>60</sup> for adsorption on copper (the results for copper will be discussed in detail below). We call this the amortization effect.

The subsequent decrease in the sticking coefficient with increasing  $\theta$  (Fig. 12) may be due to several causes. One of the main causes is thermodesorption. Evidence for this is the strong dependence of the equilibrium degree of coverage on the gas flux density. In the absence of a deficit of unoccupied adsorption sites, an equilibrium coverage was established such that the flux densities of the desorbed and incident molecules were equal. In addition, the results of the Monte Carlo simulation<sup>59</sup> with amortization, thermodesorption, and a weak lateral interaction between molecules taken into account agree satisfactorily with experiment (Fig. 12), confirming the conclusion that thermodesorption plays a governing role in the appearance of the descending branch of  $S(\theta)$ .

An extremely original interpretation of the cause of the decrease in the sticking coefficient in the region of completion of the first physisorbed monolayer of H<sub>2</sub> on the (001) surface of ruthenium was proposed by Friess, Schlichting, and Menzel.<sup>35</sup> Those authors<sup>35</sup> see the decrease in the sticking coefficient in the region  $\theta \approx 1$  as being caused by an increase in the lattice stiffness of the molecular adlayer of hydrogen owing to the lateral compression of this layer in comparison with a molecular plane of the hydrogen crystal. The driving force of this compression is the rather large difference in the binding energy of the molecules with the substrate in the first and second physisorbed layers ( $E_d$  is substantially larger in the first layer). Therefore, it is energetically more favorable for a molecule striking the surface to “squeeze” into the first monolayer than to be incorporated in the second layer. This possibility, in turn, is explained by the anomalously high compressibility of the hydrogen layer owing to the large amplitude of the zero-point vibrations of the H<sub>2</sub> molecule. Anomalous compressibility of the hydrogen crystal was reported in Ref. 61. Figure 13, which is reproduced from Ref. 35, shows the sticking

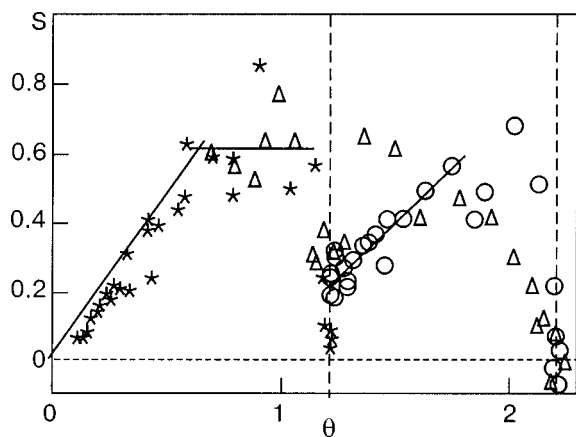


FIG. 13. Dependence of the sticking coefficient of H<sub>2</sub> on the degree of coverage on the Ru(001) surface filled beforehand with a chemisorbed monolayer.<sup>35</sup>  $\Delta$ — $T_s=4.8$  K;  $\star$ — $T_s=5.5$  K;  $\circ$ —adsorption in a second layer at  $T_s=4.8$  K.

coefficient of H<sub>2</sub> on Ru(001) as a function of the degree of coverage. It is seen that  $S$  decreases sharply upon completion of the first monolayer. In Ref. 35 two peaks were observed in the thermodesorption spectrum, corresponding to the first and second layers, at  $T_s=4.8$  K. When the adsorption temperature was increased to 5.5 K, so that the second layer was not held, one peak remained in the thermodesorption spectrum, and the  $S(\theta)$  curves in Ref. 35 and in our studies are qualitatively similar. As we have said, a Monte Carlo simulation taking thermodesorption into account but not the compressibility of the adlayer gives a satisfactory description of our experimental results,<sup>59</sup> although it cannot be ruled out that the compressibility effect may have a slight influence on the descending branch of  $S(\theta)$ . To obtain a more reliable answer to this question we are planning to conduct experiments at lower temperature, where several molecular layers will be held.

In comparing the results of our studies for the H<sub>2</sub>/W(110) system<sup>55,58,59</sup> with the results of Ref. 35 for the H<sub>2</sub>/Ru(001) system, we must address two questions. The first is, why in our case does the measured  $S(\theta)$  curve extend to  $\theta \approx 1$ , while in Ref. 35 it extends to  $\theta \approx 2$ . A possible reason for this difference is that the activation energy of H<sub>2</sub> desorption from ruthenium ( $\sim 30$  meV<sup>35</sup>) is substantially higher than that for tungsten ( $\sim 15$  meV<sup>58,59</sup>). Probably the value of  $E_d$  for the second molecular adlayer is also larger in the case of Ru(001) than for W(110). That may be the reason why our experiments do not achieve the density of the first adlayer at which the compression effect and the enhanced lattice stiffness of the adlayer can play a substantial role.

The second question pertains to the hydrogen thermodesorption spectra. Both in our studies and in Ref. 35, two main peaks of desorption of the molecular phase of adsorption are observed. However, in our case both peaks represent the desorption of a single physisorbed layer in which the molecules are found in different states.<sup>44,57</sup> In Ref. 35 each of

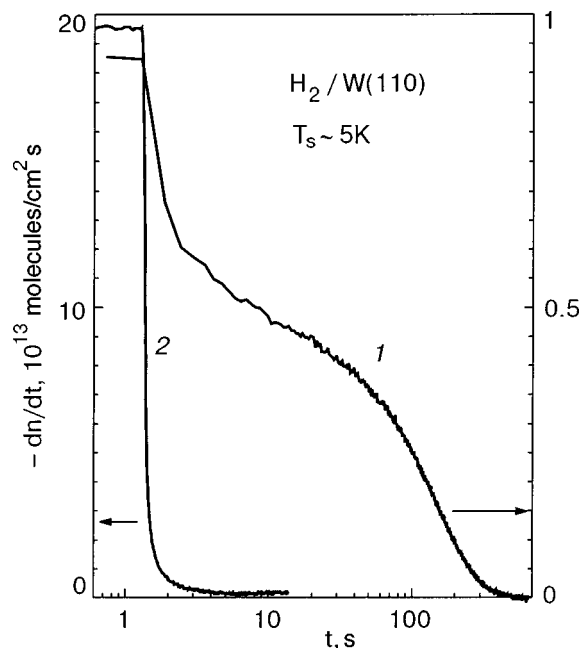


FIG. 14. Rate of isothermal desorption of H<sub>2</sub> versus time.<sup>57</sup> 1—Low flux density; 2—high flux density.

the two thermodesorption peaks represents a separate monolayer.

*3.1.2.2. Kinetics of the isothermal desorption of H<sub>2</sub> from W(110).* Since a change in the flux density of molecules onto the surface has an influence on the kinetics of the low-temperature adsorption of H<sub>2</sub> on W(110), according to the principle of detailed balance, one can expect that the desorption kinetics will also be influenced by the flux density. The results of a study of how the value of the molecular flux density in the formation of a hydrogen adlayer influences the subsequent isothermal desorption at  $T_s \sim 5$  K are reported in Refs. 44 and 57.

Figure 14, taken from Ref. 57, shows the time dependence of the rate of isothermal desorption of H<sub>2</sub> from W(110) at  $T_s \sim 5$  K from adlayers formed at flux densities of  $\sim 1 \times 10^{13}$  and  $2 \times 10^{14}$  molecules/cm<sup>2</sup>. It is seen that increasing the flux density sharply suppresses the isothermal desorption: the number of molecules desorbed at the higher flux density is smaller by approximately a factor of 50 than for the case of the lower flux density. In Refs. 44 and 57 the suppression of the isothermal desorption of H<sub>2</sub> is interpreted as being a consequence of a phase transition from a 2D gas to a 2D condensate in the adlayer. It is known that the critical size of the condensed-phase nuclei decreases with increasing supersaturation. For this reason one expects that the probability of realization of a gas–condensate phase transition during the time of an experiment increases with increasing flux density, and that is most likely what is observed. The activation energy for desorption from a 2D condensed phase should be larger than that for a 2D gas phase because of the lateral attractive interaction of the molecules. This is the reason for suppression of the isothermal desorption with increasing flux density.

At a low flux density one observes a fast stage (several seconds) and a slow stage (hundreds of seconds) of desorption. At a high flux density only the fast stage of desorption is observed. The fast stage involves the desorption of the insignificant number of molecules contained in the second molecular layer. The slow stage can be analyzed using the Polyani–Wigner equation in logarithmic form:

$$\log\left(-\frac{dn}{dt}\right) = \log \nu_d + a \log n - 0.43 \frac{E_d}{kT_s}, \quad (3.2)$$

where  $n$  is the surface density,  $\nu_d$  is a frequency factor,  $E_d$  is the activation energy for desorption, and  $a$  is the order of the desorption reaction.

Figure 15, taken from Ref. 57, shows the dependence of the rate of desorption on the density. It is seen that a large part of the adlayer is desorbed in the first order of the reaction, which is reasonably ascribed to desorption from a 2D gas phase. However, in a small interval of densities,  $10^{12}$ – $10^{13}$  molecules/cm<sup>2</sup>, the order of the reaction is close to zero. In Refs. 44 and 57 this last result is interpreted as being a consequence of the replenishment of the 2D gas phase due to “melting” of islands of the 2D condensate. Apparently, even in the case of a low flux density (during the formation of the adlayer) islands of the 2D condensate form near defects of the surface, but they contain a very insignificant fraction of the total number of molecules in the adlayer.

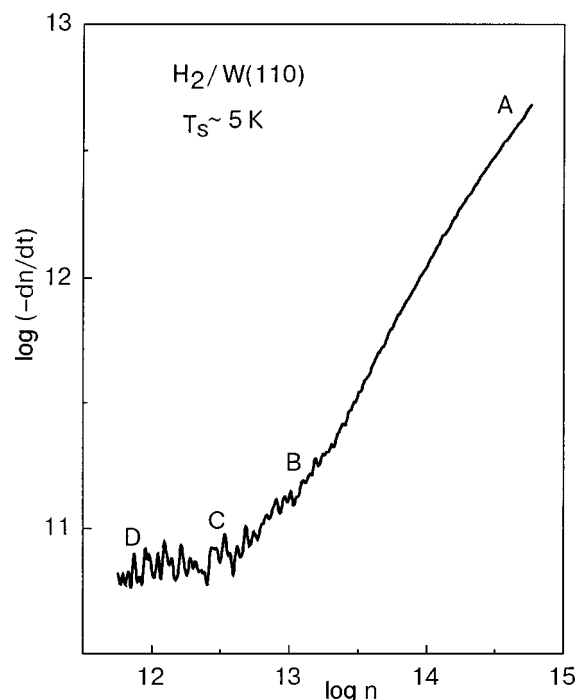


FIG. 15. Rate of isothermal desorption of H<sub>2</sub> versus density on a logarithmic scale.<sup>44,57</sup> On segment AB one has  $a \approx 1$ ; on segment CD,  $a \approx 0$ .

Evidence in favor of this interpretation comes from the thermodesorption spectra of adlayers formed at low and high flux densities. Such spectra are shown in Fig. 16.<sup>57</sup> It is seen that for a low flux density the desorbed molecules are mainly found in the 6 K (2D gas) peak and only an insignificant number of them are found in the 10 K (2D condensate) peak. In the case of the high flux density the number of molecules in the 10 K peak was tens of times larger.

Based on the results discussed, a hypothetical model of the hydrogen adlayer on W(110) at  $T_s \sim 5$  K was proposed in Refs. 44 and 57. In this model, which is illustrated in Fig. 17, the first molecular layer contains a 2D gas with neighboring islands of the 2D condensate, and the second molecular layer, in equilibrium with the intense flux, contains a quite small number of molecules, which very rapidly fly off when the incident flux is shut off.

It is of interest to elucidate the character of the transition from the 2D gas to the 2D condensate with increasing flux density of molecules onto the surface. Figure 18, taken from Ref. 57, shows the total number of isothermally desorbed H<sub>2</sub> molecules (in fractions of a monolayer) as a function of the flux density. Up to a flux density of  $\sim 1 \times 10^{14}$  molecules/cm<sup>2</sup> the experimental points fall on the Langmuir isotherm.<sup>62</sup> This means that at such flux densities there are no substantial changes in the adlayer. However, at a flux density of  $2 \times 10^{14}$  molecules/cm<sup>2</sup> the number of desorbed molecules falls off sharply. Thus there exists a critical value of the flux density (supersaturation) that must be exceeded for the phase transition from the 2D gas to the 2D condensate to occur.

We conclude this paragraph by noting that appreciable isothermal desorption of deuterium at  $T_s \sim 5$  K is not observed. We attribute this circumstance to the deeper position

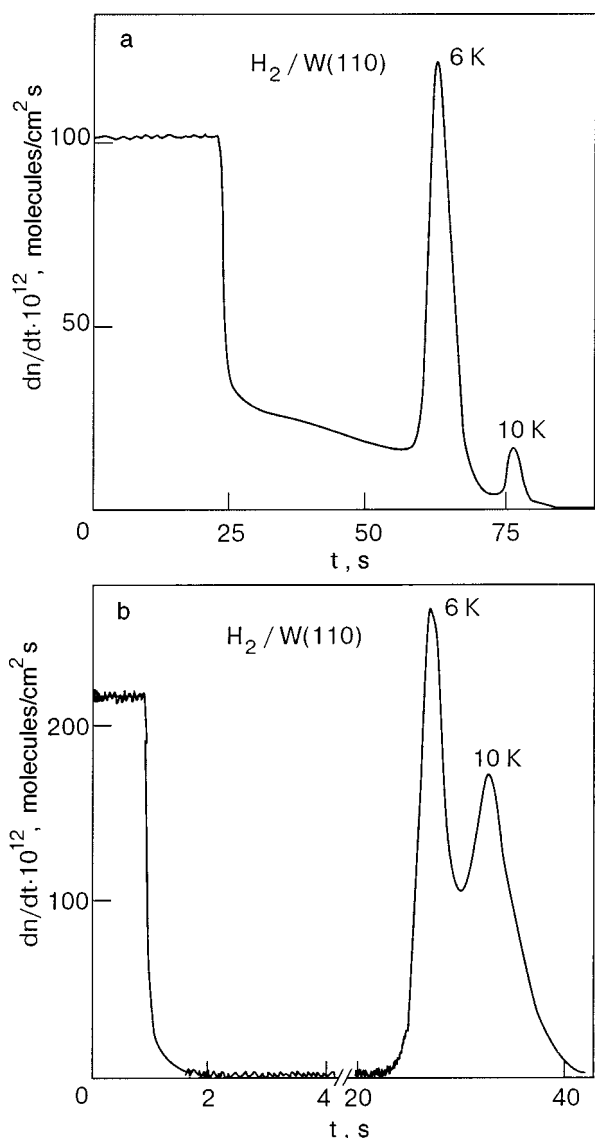


FIG. 16. Thermodesorption spectra for low (a) and high (b) flux densities.<sup>44,57</sup>

of the level of zero-point vibrations of the heavier  $D_2$  molecule in the physisorption potential well.

3.1.2.3. Features of the adsorption kinetics of hydrogen on the Mo(110) surface at  $T_s \sim 5$  K. The Mo(110) surface has an atomic structure that is practically identical to that of W(110), but the electronic structure of these metals is somewhat different. It is of interest to compare the kinetics of  $H_2$  adsorption on these surfaces. Figure 19, taken from Ref. 57, shows the sticking coefficient of  $H_2$  and  $D_2$  on the Mo(110) surface as a function of coverage. The very weak variation of the sticking coefficient in the initial stage of the adsorption

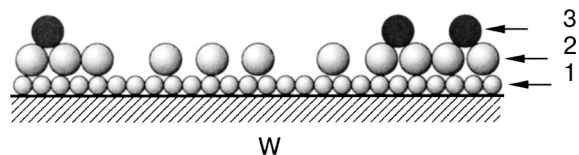


FIG. 17. Model of a hydrogen adlayer at  $T_s \approx 5$  K.<sup>57</sup> 1—Monolayer of chemisorbed atoms; 2—monolayer of physisorbed molecules in the form of a 2D gas and a 2D condensate; 3—polylayer condensation.

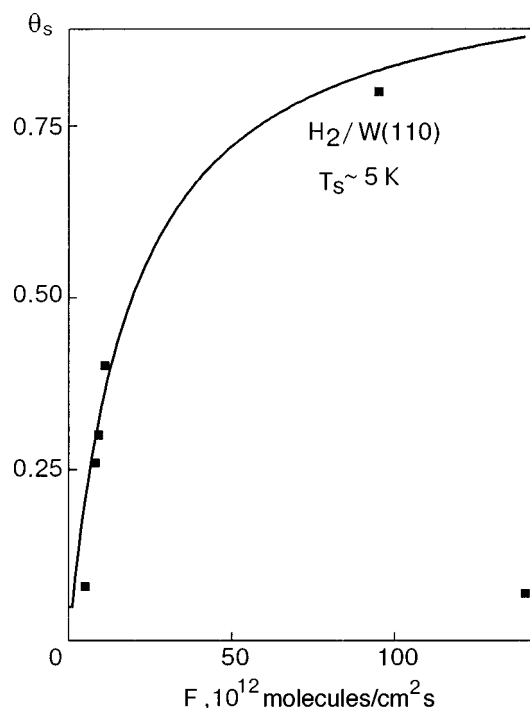


FIG. 18. Langmuir isotherm.<sup>57</sup> ■—Experimental points.

process (for  $D_2$  it is practically constant) is evidence of a mechanism of adsorption via an extrinsic precursor state, unlike that which is observed for W(110) (see Sec. 3.1.1, Fig. 8). As we have said, the absence of appreciable growth of the sticking coefficient indicates that hydrogen (deuterium) initially accumulates on the surface in atomic and not molecular form. One notices a sharp and deep minimum near  $\theta=0.5$  for hydrogen, which corresponds to a monolayer of chemisorbed atoms.

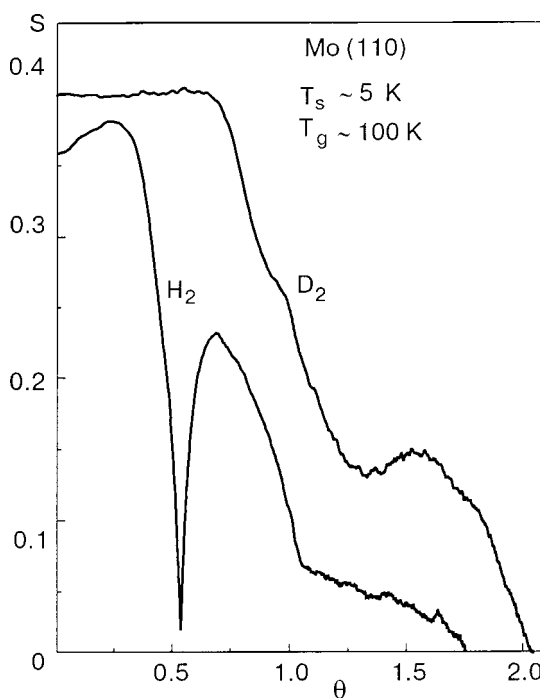


FIG. 19. Sticking coefficient for  $H_2$  and  $D_2$  on Mo(110) versus the degree of coverage.<sup>49,57</sup>

The following explanation for this feature was proposed in Refs. 49 and 57. Up until the layer of chemisorbed atoms is practically complete, the  $H_2$  molecules, owing to their anomalously high mobility on the layer of adatoms, find unoccupied parts of the surface and are dissociatively chemisorbed. Once filled with a chemisorbed monolayer of atoms, the surface becomes inert (the unsaturated valence bonds are exhausted), and the sticking coefficient falls catastrophically. Since the temperature is low enough for a physisorbed molecular layer to be held, weakly bound molecules begin to accumulate on the surface, the accommodation improves, and the sticking coefficient increases.

One might well ask why this feature is not observed in the case of deuterium adsorption. We assume that once again the cause lies in the difference of the quantum properties of the  $D_2$  molecule. The deeper position of the level of zero-point vibrations (in comparison with hydrogen) makes for a better-developed potential relief and lower mobility of the molecules. Therefore,  $D_2$  molecules begin to accumulate on the surface even before completion of the chemisorbed atomic phase, and that compensates the decrease in the sticking coefficient caused by the lowering of the chemical activity of the surface. We do not rule out the possibility that the quantum diffusion of molecules plays some role in the formation of the feature on the  $S(\theta)$  curve for  $H_2/\text{Mo}(100)$ . To check this possibility one must lower the sample temperature.

### 3.1.3. Structure of the hydrogen adlayer at $T_s \approx 5$ K

The structure of hydrogen adfilms on the transition metals W, Mo, and Ni at  $T_s \sim 5$  K has been studied by the LEED method by Fedorus and co-workers.<sup>63–68</sup> Some of the results of those studies have been discussed in the review by Naumovets.<sup>9</sup> The main and most reliable data pertain to the structure of an atomic chemisorbed layer, obtained by annealing a hydrogen adlayer formed at  $T_s \sim 5$  K, on the close-packed (110) faces of tungsten and molybdenum. Adsorption at  $T_s \sim 5$  K leads to the formation of an almost completely disordered layer, although the authors of Refs. 63 and 68 discern in the diffraction patterns a slight manifestation of some sort of order. As was shown in Refs. 34, 44, 46–49, and 57, on the W(110) and Mo(110) surfaces at  $T_s \sim 5$  K a monolayer of chemisorbed atoms is formed, with a molecular physisorbed layer formed on top of it. An analogous result was obtained in Ref. 35 for the adsorption of hydrogen on the surface of ruthenium. Clearly, for such a composite adlayer it is scarcely possible to interpret the LEED patterns reliably.

Clear and well-interpretable LEED patterns for the system of hydrogen on W(110) are obtained after an adlayer formed at  $T_s \sim 5$  K is annealed at 120–160 K. After the annealing the sample was again cooled to 5 K, and the structures  $p(2 \times 1)$ ,  $(2 \times 2)$ , and  $(1 \times 1)$  were observed for coverages of  $\theta = 0.5$ ,  $\theta = 0.75$ , and  $\theta = 1$ , respectively. Models of the first two structures are shown in Fig. 20, taken from Ref. 63. Also shown in this figure are the intensities of the reflections of these structures as functions of the substrate temperature. It is seen that an order–disorder phase transition occurs at temperatures significantly below room temperature, and the transition temperature is higher for the  $(2 \times 2)$  struc-

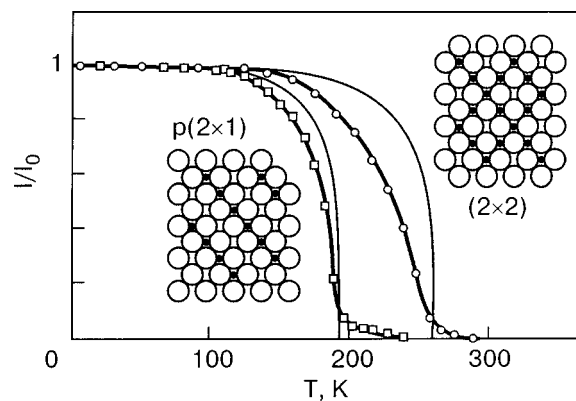


FIG. 20. Temperature dependence of the intensity of the diffraction peaks for the  $p(2 \times 1)$  and  $(2 \times 2)$  structures of hydrogen on W(110);<sup>63</sup> the fine lines show an Ising model calculation.

ture than for  $p(2 \times 1)$ , a circumstance which is explained by the stronger interaction of the hydrogen adatoms in the more densely packed structure. Lyuksyutov and Fedorus<sup>20</sup> did a detailed study of the order–disorder transitions in the structures  $p(2 \times 1)$  and  $(2 \times 2)$ ; they established that the temperature dependence of the intensities of the corresponding reflections obeys a power law and determined the critical exponents  $\beta = 0.13$  for  $p(2 \times 1)$  and  $\beta = 0.25$  for  $(2 \times 2)$ . For hydrogen on the Mo(110) surface the  $p(2 \times 1)$  structure was not observed, but only the  $(2 \times 2)$  structure at a degree of coverage  $\theta = 0.5$ , and the authors of Ref. 64 proposed a model for such a structure.

Fedorus and co-workers observed an electron-stimulated disordering (ESD) effect in a chemisorbed hydrogen layer at  $T_s \sim 5$  K on the W(110) surface<sup>63</sup> and on the Mo(110) surface,<sup>64</sup> and then an electron-stimulated ordering (ESO) effect<sup>64,66</sup> as well. It was shown in Ref. 66 that in both the ESD and ESO effects the degree of order tends with time to the same level of incomplete ordering, which suggests a universality of the mechanisms of ESD and ESO. The cause of the incomplete ESD is the competing ESO effect. Typically, in the case of adsorption on W(110) the ESD reaches a significantly higher degree than in the case of adsorption on Mo(110).<sup>65</sup> This difference can be explained by the substantially lower mobility of adatoms on W(110) (the greater depth of the potential relief along the surface). One can discern a certain analogy between this difference in the behavior of hydrogen films on W(110) and Mo(110) and the difference in the kinetics of hydrogen adsorption on these substrates.<sup>49</sup> The ESD and ESO effects were subsequently investigated in detail, and a mechanism for them was proposed.<sup>64–69</sup> One of the most likely mechanisms involves the excitation of vibrational states of the hydrogen adatoms, which can migrate along the surface, bringing about a higher mobility of the adatoms. Because of the low mass of the hydrogen atom, high-frequency vibrations are excited, which are long-lived because of the inefficient energy exchange with the substrate.<sup>69</sup>

Let us say a few words about isotope effects in the structure of hydrogen adfilms. Adlayers of H, D, and H+D on W(110) are characterized by the same set of structures:  $p(2 \times 1)$ ,  $(2 \times 2)$ , and  $(1 \times 1)$ ; an isotope effect in the order–disorder phase transitions is not observed: films of H, D, and

H+D disorder at practically the same temperatures.<sup>65</sup> However, a strong isotope effect is observed in the rate of ESD: in deuterium films the ESD occurs one-fifth as fast as in hydrogen films.<sup>65,66</sup>

A characteristic feature of the ESD of hydrogen and deuterium adlayers is the absence of an energy threshold: the effect occurs even at thermal energies of the electrons.<sup>65–68</sup> This is explained by the fact that when the electron strikes the surface, an energy of  $\sim 5$  eV (the difference between the vacuum level and the Fermi level of the metal) is released, and that energy is expended on excitation of vibrations of an adatom. The authors of Ref. 65 point out several signs of quantum diffusion in the molecular phase. It should be noted, however, that at degrees of coverage  $\theta < 1$  (in atoms) practically all the hydrogen is contained in an atomic chemisorbed phase, especially for the Mo(110) surface,<sup>49</sup> and the facts observed in Ref. 65 can scarcely be applied to the molecular phase. In the opinion of the authors of Ref. 65, the conclusion reached in the paper by Di Foggio and Gomer<sup>70</sup> that tunneling diffusion of hydrogen adatoms on W occurs at  $T_s < 140$  K is mistaken.

Some information about the structure of a hydrogen adlayer at  $T_s \approx 5$  K can be obtained from studies by the static skin-effect method.<sup>71–79</sup> Since Panchenko and coauthors have recently published a review devoted to galvanomagnetic size effects, of which the static skin effect is one,<sup>8</sup> there is no need to present a detailed description of this method here. However, in order to achieve a certain independence of this review article we shall not simply refer the reader to that review<sup>8</sup> but will give a brief account of the essence of the method and the experimental results only insofar as they pertain to the structure of an adsorbed hydrogen layer.

If a single-crystal slab of a pure metal is cooled to a temperature of  $\sim 5$  K and placed in a sufficiently strong magnetic field directed parallel to the surface of the slab, for example, the conductivity of the slab will be determined by a narrow subsurface layer (with a thickness of the order of the Larmor radius), since the deeper layers will be “magnetized.” This is a consequence of the fact that electrons colliding with the surface have the opportunity to propagate a distance of the order of the mean free path, and their contribution to the conductivity will be the greater the higher the degree of specularly of their reflection.<sup>8</sup>

According to the ideas set forth in the article by Andreev,<sup>74</sup> the reflection of conduction electrons by the surface of a metal is governed by diffraction effects on the outermost atomic layer. Therefore, the character of the reflection of electrons depends on the structure of this outermost layer. The reflection of electrons should also be influenced by the structure of an adsorbed layer. This has been confirmed in the experiments by Panchenko and co-workers:<sup>23,25,72,74,75</sup> the adsorption of a disordered monolayer (oxygen) led to a twofold increase in the magnetoresistance of a tungsten slab with a (110) surface.

The influence of an ordered monolayer of hydrogen on the magnetoresistance of a tungsten slab with the (110) surface was investigated in Ref. 25 using a device which combined the method of the static skin effect with the LEED method (Fig. 4). The LEED method gave the same sequence of structures with changing coverage as in the papers by

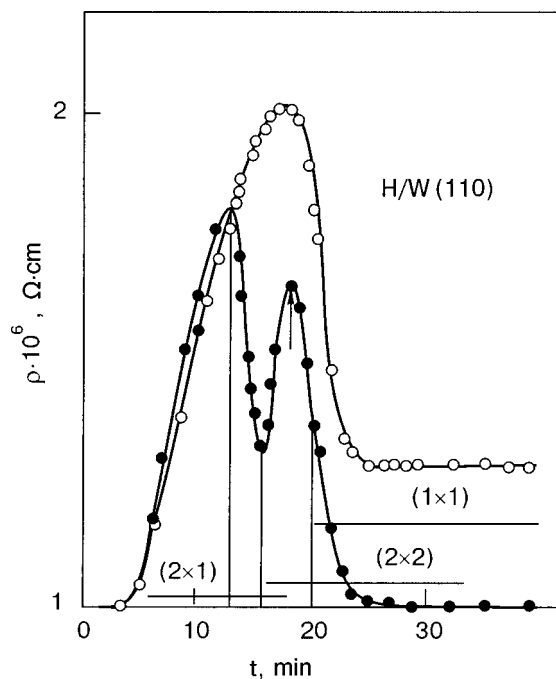


FIG. 21. Dependence of the magnetoresistance of a W(110) slab on the exposure time in hydrogen.<sup>8,25</sup> ○—adsorption at  $T_s = 4.2$  K; ●—annealing to 200 K; the vertical lines are the boundaries of the existence regions of the structures.

Fedorus and coauthors:  $p(2 \times 1)$ ,  $(2 \times 2)$ , and  $(1 \times 1)$ .<sup>63</sup> In the process of adsorption at 5 K the diffraction patterns are smeared out; the reflections become distinct after a brief annealing to  $T \sim 200$  K. Figure 21, taken from Ref. 25, shows the time dependence of the magnetoresistance of a W(110) slab after the adsorption of hydrogen at  $T_s \sim 5$  K and after annealing. After adsorption on the cooled substrate the resistance initially increases, as a result of the random distribution of the adatoms, and then decreases, reaching a certain steady level. This decrease is apparently due to the partial ordering of the adlayer, while the steady level indicates that a limiting degree of order has been attained. Thus an ordering process occurs even at  $T_s \sim 5$  K. After annealing, the initial part of the curve is nearly the same as before, but then a deep minimum, corresponding to the maximum development of the  $p(2 \times 1)$  structure, appears. After that the resistance again rises, falls, passes through a second maximum, and reaches the value characteristic for the pure substrate upon the formation of the  $(1 \times 1)$  structure. Thus the leading role is played by the symmetry and not by the chemical nature of the surface layer. The analysis of the possible electronic transitions between different parts of the Fermi surface in Ref. 25 explains the sharp decrease of the resistance upon the formation of the  $p(2 \times 1)$  structure and its growth upon the formation of the  $(2 \times 2)$  structure as being due to the switching on of electron–hole transfers.

Since the magnetoresistance of a slab is sensitive to the degree of order in an adsorbed layer, Panchenko and co-workers, after studying the dependence of the resistance of a slab with a saturated adlayer of hydrogen (deuterium) adsorbed at 5 K on the annealing time in the temperature interval 160–190 K, estimated the activation energy and the diffusion coefficient of atomic hydrogen and deuterium.<sup>77</sup> The authors were convinced that the surface diffusion of atomic

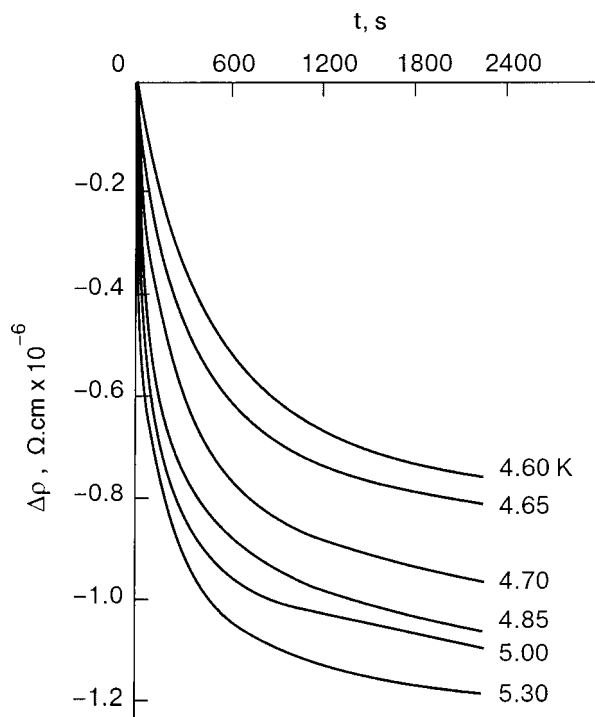


FIG. 22. Magnetoresistance of a W(110) slab with a fixed density of  $H_2$  versus the annealing time at various  $T_s$  (Refs. 8 and 78).

hydrogen on the W(110) face is of a thermally activated character, contrary to the conclusions of Di Foggio and Gomer that the diffusion of atomic hydrogen was of a quantum nature.<sup>70</sup> The activation energy was estimated as 0.33 eV for hydrogen and 0.35 eV for deuterium.

Studies by the static skin-effect method made it possible for Panchenko and co-workers<sup>8,78</sup> to observe the kinetics of the transition to the first (atomic) layer by hydrogen (deuterium) molecules adsorbed in the second layer in the form of an extrinsic precursor state for dissociative chemisorption. It was found that the slow decrease of the magnetoresistance on the descending branch of its time dependence continues after the surface is no longer accessible to the gas. This is shown for the system  $H_2/W(110)$  in Fig. 22, which is taken from Ref. 8. The authors of Refs. 8 and 78 assumed with complete justification that the cause of the decrease in the resistance is the increase in the area of the islands of the  $(1 \times 1)$  atomic phase due to the diffusion of molecules toward the edge of the island and their transition to the first layer, accompanied by dissociation. A similar relaxation of the magnetoresistance has also been observed for the systems  $H_2/Mo(110)$ ,  $H_2/W(110)$ , and  $D_2/W(110)$ . Measurement of the temperature dependence of the rate of decrease of the resistance allowed the authors of Refs. 8 and 78 to estimate the activation energy for surface diffusion of molecules over the chemisorbed atomic layer:  $E_m = 6.4 \pm 0.7$  meV for  $D_2/W(110)$ ,  $2.7 \pm 0.5$  meV for  $H_2/W(110)$ ,  $1.1 \pm 0.2$  meV for  $D_2/Mo(110)$ , and  $0.8 \pm 0.2$  meV for  $H_2/Mo(110)$ . A significant isotope effect in the surface diffusion was explained by the authors of Ref. 8 as being due to the difference in the position of the levels of the zero-point vibrations of the  $H_2$  and  $D_2$  molecules, as in the explanations for the isotope effects in Refs. 44, 49, 55, and 57. It can be thought that the very small value of  $E_m$  for  $H_2/Mo(110)$  compared

to those for  $D_2/Mo(110)$  and  $H_2/W(110)$  is manifested in the appearance of a sharp feature on the  $S(\theta)$  curve for the first system.<sup>49,57</sup>

Studies by Panchenko and co-workers<sup>79</sup> of the adsorption of deuterium on the W(100) surface by the static skin-effect method revealed certain differences from the  $D_2/W(110)$  system. It was found that relaxation of the magnetoresistance is not observed after the  $D_2$  flux is shut off at 4.2 K. This circumstance was explained by the authors as being due to the absence of islands of the ordered atomic phase  $c(2 \times 2)$  on that surface at 4.2 K. In my opinion this may also be caused by the hindered surface diffusion of  $D_2$  molecules over the layer of atomic deuterium on W(100) in comparison with W(110). In addition, the value estimated in Ref. 79 for the activation energy of the ordering process in the atomic phase turned out to be substantially larger than for W(110):  $\sim 0.6$  eV as compared to  $\sim 0.3$  eV.<sup>77</sup>

### 3.2. Adsorption of hydrogen on noble metals

#### 3.2.1. State of adsorbed particles

As was mentioned in Sec. 1.2, in the interaction of an incident hydrogen molecule with the surface of copper or another noble metal, the presence of the Pauli repulsion gives rise to an appreciable activation barrier on the path of the molecule toward dissociation, and this barrier can be overcome only if the incident molecule has sufficient kinetic energy. This fact has been confirmed by many experiments with monoenergetic molecular beams (see, e.g., Refs. 80–83). For  $H_2$  a kinetic energy  $> 200$  meV must be imparted to the molecules for the adsorption to become noticeable.<sup>82</sup> Thus for beams with ordinary thermal energies and at the usual substrate temperatures there is no noticeable adsorption of hydrogen on the surface of copper.

The situation is radically altered in the case of deep cooling of the sample. Here a state of physisorption becomes stable, and hydrogen accumulates on the surface. The physisorption of hydrogen (deuterium) on the surface of noble metals silver and copper upon their cooling by liquid helium was first reliably detected by Avouris *et al.*<sup>27</sup> and by Andersson and Harris.<sup>28</sup> Using the HREELS method, the authors of those papers<sup>27,28</sup> observed a very slight difference in the spectra of the characteristic energy loss to rotational and rotational–vibrational excitations in physisorbed molecules in comparison with those in the gas phase. This was evidence that the state of physisorption is close to the state of the free molecule and that the physisorbed molecule behaves as an almost unhindered rotator. Such behavior of  $H_2$  molecules physisorbed on silver has also been observed in Ref. 84.

In Refs. 27 and 28 some contradictory data were obtained as to conversion of *o*- $H_2$  into *p*- $H_2$  as a result of adsorption. In Ref. 27 the conversion of *o*- $H_2$  into *p*- $H_2$  in the physisorbed state was reported. In Ref. 28, on the contrary, no appreciable *o*–*p* conversion in the physisorbed layer was observed during the time of the experiment. Granted, in a later study<sup>85</sup> Svensson and Andersson observed *o*–*p* conversion in a physisorbed layer on the same Cu(100) surface at a rate of approximately 1 monolayer in 4 min. The authors did not offer a clear explanation for the cause of the difference in the results of Refs. 28 and 85 but suggested that the Cu(100) samples in Refs. 28 and 85 could somehow

differ in structure or by the presence of impurities. An attempt to explain the difference in the rate of  $o$ - $p$  conversion on different surfaces by invoking a mechanism of virtual exchange of an electron between the metal and an antibonding orbital of the molecule was made by Iliska.<sup>86</sup>

The authors of Ref. 28 found that the relative occupations of the  $o$  and  $p$  states of hydrogen in a physisorbed layer differ substantially from those in the gas phase: whereas in the gas phase at 300 K the population ratio  $o$ - $H_2$ :  $p$ - $H_2$  is equal to 3, in a physisorbed layer this ratio turned out to be 1.4. In the opinion of the authors of Ref. 28, this is evidence of a predominant adsorption of  $p$ - $H_2$ , with  $j=0$ , in comparison with  $o$ - $H_2$ , with  $j=1$ .

Andersson and Harris made a more detailed study<sup>87</sup> of the influence of the rotational state of the hydrogen gas ( $n$ - $H_2$ ,  $p$ - $H_2$ ,  $D_2$ , HD) on the sticking probability for a Cu(100) surface cooled to 10 K. As a measure of the adsorption they used the intensities of the corresponding peaks in the spectrum of EELS and also the change in the work function. The authors of Ref. 87 found that the ratio of the sticking coefficients of  $p$ - $H_2$  and  $n$ - $H_2$  equals 1.4, i.e., molecules with  $j=0$  are adsorbed with a higher probability than are molecules with  $j=1$ . The authors of Ref. 87 also came to the conclusion that a large part of the kinetic energy of the molecule upon impact with the surface is converted into rotational energy.

Information about how the rotational state of the incident hydrogen molecules influences the sticking probability is also found in a number of other papers (see, e.g., Refs. 52–54 and 88), although for higher  $T_s$  and other substrates (Pd, Pt, Rh). Incidentally, the authors of those papers assume that the influence of the rotational state on the sticking coefficient is proof of the realization of the dynamic steering mechanism<sup>50,51</sup> and of the unimportant role of adsorption via a precursor state.

Thus, on the surface of noble metals upon deep cooling a physisorbed film of hydrogen (deuterium) forms which is in direct contact with the surface atoms of the metal. For transition metals at helium temperatures, on the other hand, first a monolayer of chemisorbed atoms forms on the surface and then a physisorbed layer of molecules forms on top of that monolayer (Sec. 3.1).

### 3.2.2. Adsorption kinetics

**3.2.2.1. Dependence of the sticking coefficient on the degree of coverage.** Since in the adsorption of hydrogen on copper, dissociation of molecules incident at moderate thermal velocities does not occur, the initial sticking coefficient (at zero coverage) is very small. The reason for this is the enormous mass difference of the colliding partners and, as a consequence, the small accommodation coefficient. However, as physisorbed molecules accumulate on the surface it becomes increasingly probable for an incident molecule to collide with a previously adsorbed molecule, which has an equal mass.<sup>30,60</sup> Figure 23, taken from Ref. 30, shows the sticking coefficient of deuterium on the Cu(100) surface at  $T_s \sim 10$  K as a function of the degree of coverage. In Ref. 30 the experimental dependence obtained is written in the form

$$S = S_0(1 - \theta) + S_1 \theta, \quad (3.3)$$

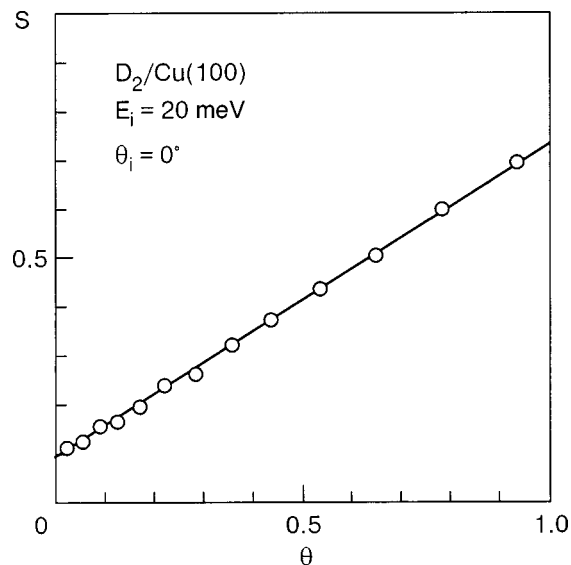


FIG. 23. Sticking coefficient for  $D_2$  on the Cu(100) surface at  $T_s \sim 10$  K versus the degree of coverage.<sup>30</sup>  $E_i$  is the energy of the incident molecules, and  $\theta_i$  is the angle of incidence.

where  $S_0$  and  $S_1$  are the sticking probabilities of a molecule in collision with the clean surface and with a previously adsorbed molecule, respectively. For the particular system  $D_2$ /Cu(100) the value of  $S_1$  is approximately 8 times larger than  $S_0$ . In the case of copper this sort of amortization effect is observed starting at zero coverage, whereas in the case of the transition metals tungsten and molybdenum this effect is manifested in the region of completion of a chemisorbed atomic phase (paragraphs 3.1.2.1 and 3.1.2.3).

**3.2.2.2. Dependence of the initial sticking coefficient on the energy and angle of incidence of the molecules.** Important and interesting features of the sticking of hydrogen molecules to the copper surface are revealed by studying the influence of the energy  $E_i$  and angle of incidence of a molecular beam on the initial sticking coefficient. The main contribution to the investigation of this question was made by group of investigators from Chalmers University of Technology in Göteborg, Sweden. The combination of precision experiments with monoenergetic molecular beams of  $H_2$  and  $D_2$  and theoretical calculations permitted the authors of Refs. 30 and 89 to create an extremely complete and complex picture of the interaction of hydrogen and deuterium molecules with the surface of a metal single crystal.

The authors of Refs. 30 and 89 showed by comparison of the experimental results with the results of theoretical calculations that the sticking process for a molecule in the physisorption potential well cannot be interpreted on the basis of a purely classical model, which predicts that the sticking coefficient of a light inert particle (in the case of hydrogen, without dissociation) in the limit of zero energy must equal unity and decrease to zero at an energy of the incident particles of several millielectron-volts. However, the experiment shows that the sticking coefficient of hydrogen (deuterium) on the Cu(100) surface varies from  $\sim 0.2$  to a very small value in the energy range 0–30 meV, which is approximately equal to the width of the phonon bands. Such behavior of the sticking coefficient agrees with quantum calculations in the forced-oscillator model (FOM) or in the distorted-wave Born



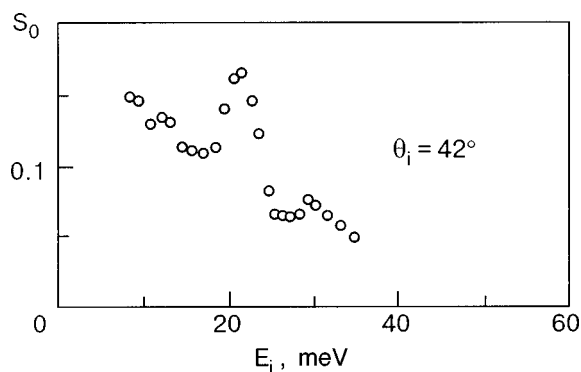


FIG. 24. Initial sticking coefficient for  $H_2$  on Cu(100) at  $T_s \sim 10$  K versus the energy of the molecules.<sup>30</sup>

approximation (DWBA). At low energies of the molecules a one-phonon process occurs, and at high energies a multiphonon process. Thus these results attest to the important role of the quantum mechanism of sticking for light inert particles.

According to Refs. 30 and 89, the sticking of molecules occurs with the participation of a normal and a resonance process. The normal process includes trapping of the particle after the first impact on account of inelastic scattering on the phonon system; this gives a contribution to the so-called background sticking. The probability of such sticking decreases smoothly with increasing  $E_i$  within the width of the phonon bands. Figure 24, taken from Ref. 30, shows the experimental dependence  $S_0(E_i)$  for an angle of incidence of  $42^\circ$  relative to the normal. The  $S_0(E_i)$  curves exhibit a sharp peak at a molecular energy of  $\sim 20$  meV and a less noticeable peak at  $E_i \approx 25$  meV. According to the interpretation of those authors,<sup>30,89</sup> the main cause of the peaks is the trapping of a molecule into a quasibound state on the surface under resonance excitation of the rotational states of the molecule. Probably a transformation of the kinetic energy of the molecule into rotational energy occurs here which is accompanied by a decrease in the translational velocity and makes for a higher sticking probability. Although in itself the excitation of rotational states can have a negative effect on the sticking probability,<sup>28,52–54</sup> the decrease in the translational velocity has a greater positive effect.

A molecule in a quasibound state (with positive total energy) moves rather freely along the surface and can ultimately either stick as a result of excitation of a phonon or be ejected back into the vacuum as a result of diffraction on the lattice of surface atoms of the substrate.<sup>30,89</sup> In general diffraction effects, according to Refs. 30 and 89, play an extremely important role in the mechanism of sticking in the physisorption potential well. As to the subsequent fate of a physisorbed molecule, it can also be ejected into the vacuum as a result of a thermodesorption process if the substrate temperature is high enough to foster an appreciable desorption rate. As was shown in Sec. 3.1, thermodesorption has a substantial influence on the sticking coefficient of hydrogen on the surface of tungsten at  $T_s \sim 5$  K.

Besides sticking, the authors of Refs. 30 and 89 also studied the scattering of molecules by the surface and observed a clear correlation of those processes.

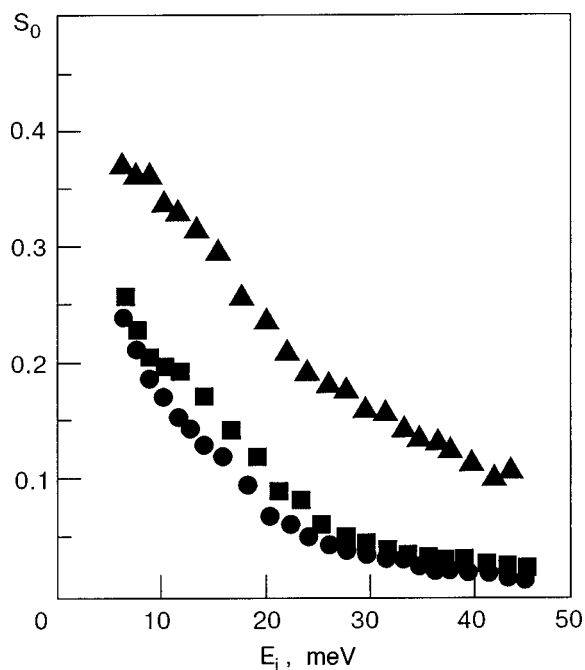


FIG. 25. Initial sticking coefficient for  $D_2$  on Cu(111) ( $\bullet$ ), Cu(100) ( $\blacksquare$ ), and Cu(110) ( $\blacktriangle$ ) at  $T_s \sim 10$  K versus the energy of the molecules at normal incidence.<sup>89</sup>

### 3.2.3. Influence of the structure of the surface on adsorption

The Chalmers research group also devoted considerable attention to the influence of the structure of the surface of the crystal on the parameters of the physisorption of hydrogen. Experiments and theoretical calculations were carried out for the low-index faces of copper<sup>89–92</sup> and aluminum.<sup>92</sup> Figure 25, taken from Ref. 89, shows the dependence of  $S_0$  on  $E_i$  for normal incidence of the beam. It is seen that in the energy range 5–45 meV the initial sticking coefficient (in this case for deuterium) is substantially larger on the less densely packed face (110) than on the more densely packed faces (111) and (100). DWBA theory for a one-phonon mechanism of energy transfer from the molecule to the substrate explains the observed tendency. A comparison of the experimental and theoretical results permits the conclusion<sup>89,90</sup> that the observed differences in the sticking probability on the non-close-packed and close-packed faces are caused by structurally specific differences in the molecule–phonon interaction. The transfer of energy is more efficient, and, hence, the sticking is more intense, on a non-close-packed surface, with a larger surface unit cell (and, accordingly, a smaller reciprocal lattice vector).

In Refs. 91 and 92 those same authors studied the influence of the crystallographic orientation (structure) of the surface on the binding energy of physisorbed  $H_2$  and  $D_2$  molecules. It was shown<sup>91</sup> that for adsorption on copper the depth of the physisorption potential well decreases on faces in the sequence (110)  $\rightarrow$  (100)  $\rightarrow$  (111), a fact which, in the words of the authors, contradicts the usual concepts of the existing theory. The contradiction is eliminated if the profiles of the electron density and their dynamic response, which depend on the face, are taken into account; the latter, in the case of the open (110) face, makes for a larger contribution to the physisorption potential from the van der Waals attrac-

tion than from the Pauli repulsion. In Ref. 92 aluminum, which also has a face-centered lattice, was investigated as a substrate as well as copper. In the case of aluminum the influence of the surface structure is more pronounced in relation to the binding energy. It was found that for the Al(111) and Al(110) faces the depths of the physisorption potential well are close to each other and 40% larger than the well depth for the Al(100) face. For a more rigorous interpretation of the effects observed, the authors of Ref. 92 consider it necessary to construct a theory on a more fundamental level.

### 3.2.4. Spectra of excitation of rotational states of physisorbed hydrogen

In the papers by the Chalmers group significant attention is paid to the spectra of rotational states of physisorbed hydrogen, which were obtained by the HREELS method.<sup>85</sup> It was found that the intensities of the peaks of the characteristic energy loss to rotational excitation of molecules of *o*-H<sub>2</sub> ( $j=1 \rightarrow 3$ ) and *p*-H<sub>2</sub> ( $j=0 \rightarrow 2$ ) molecules physisorbed at  $T_s \sim 10$  K on Cu(100) are in inverse relation to the ratio of the densities of these molecules in the gas phase. This effect is explained by an accelerated ortho-para conversion of H<sub>2</sub> in the adsorbed state as compared to the gas phase.

Very interesting features of the adsorption properties of the H<sub>2</sub> molecule have been revealed the research of the Chalmers group in studies of the rotational states of molecules adsorbed on the terraced Cu(510) face.<sup>93,94</sup> By combining measurements by the HREELS method and calculations of the total energy by the density-functional approach, the authors of Refs. 93 and 94 found unusual adsorption properties of a hydrogen molecule occupying a site above a copper atom at the edge of a step. The energies of rotational-vibrational transitions turned out to be close to those for the ideal two-dimensional quantum rotator, and the internal vibrations of the molecule are dipole-active and are characterized by an extraordinarily small energy. This last circumstance and also the fact that the Cu-H<sub>2</sub> bond length is shortened considerably while the H-H bond length in the molecule is lengthened are the characteristic signs of chemisorption. However, the fact that the energy of adsorption of the H<sub>2</sub> molecule in this state is less than 100 meV is characteristic of physisorption. The reason that the intramolecular bond is perturbed, as in the case of chemisorption, while the binding energy of the molecule with the surface is small, is seen by the authors of Refs. 93 and 94 as being due to the very high energy of zero-point vibrations of the molecule in the narrow and anharmonic potential well over a copper atom located at the edge of a step.

Calculations by the authors of Refs. 93 and 94 have also shown the existence of strong orientational anisotropy, which constrains a molecule above a single copper atom on a step to rotate in the plane perpendicular to the direction of the H<sub>2</sub>-Cu bond. This explains why an H<sub>2</sub> molecule in such a state behaves as an almost ideal 2D rotator. Unlike adsorption on the smooth Cu(100) face, when an accelerated *o*-*p*-H<sub>2</sub> conversion is observed and the adsorption states of parahydrogen are predominantly occupied,<sup>85</sup> on the terraced Cu(510) face one observes a sharp enrichment of the adsorbed layer in orthohydrogen. A similar enrichment was observed in Refs. 93 and 94 at a somewhat higher (up to

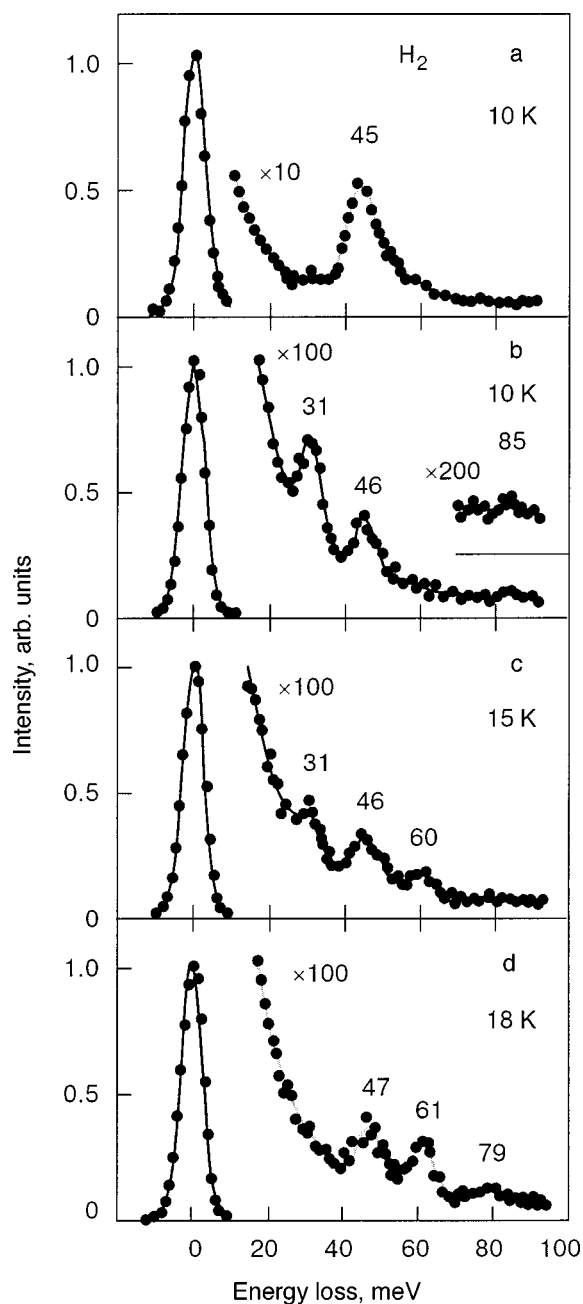


FIG. 26. Characteristic electron energy loss spectra for H<sub>2</sub> on Cu(510).<sup>94</sup> Complete monolayer at 10 K (a); steps coated at different  $T_s$  (b-d).

$\sim 18$  K) temperature. At such a temperature the density of H<sub>2</sub> molecules on the terraces becomes negligible, and all of the hydrogen is concentrated at special adsorption sites above copper atoms on the edge of a step.

As is seen in Fig. 26, taken from Ref. 94, the peaks of the electron energy loss spectrum at 31 and 46 meV, which, according to theoretical calculations, pertain to the  $0 \rightarrow 2$  rotational transitions of the two-dimensional and three-dimensional *p*-H<sub>2</sub> rotators, respectively, are present in the spectrum at a substrate temperature of 10 K. At 16 K the intensity of the 31 meV peak is significantly lower, and at 18 K this peak has vanished completely, and a pronounced peak at 61 meV, corresponding to the 2D rotational transition  $1 \rightarrow 3$  for *o*-H<sub>2</sub>, has appeared.

### 3.2.5. Photodesorption of physisorbed hydrogen

The Chalmers group has also done research on photodesorption of physisorbed hydrogen under infrared radiation. The desorption of hydrogen from vacuum cryopanel, initiated by the thermal radiation from the walls of the chamber, was noted quite some time ago.<sup>95</sup> Subsequent studies<sup>96–98</sup> confirmed the existence of such desorption, and the results of those studies indicate a nonthermal character of the process. The authors of Refs. 96 and 98 assumed that the desorption of a molecule is initiated by a phonon arising upon the absorption of an infrared photon in the substrate, after which the energy of the phonon is transferred to an adsorbed molecule.

Another point of view as to the mechanism of photodesorption was stated in Ref. 99: direct photodesorption via excitation of the molecule from the lowest vibrational level in the physisorption potential well to a state of the continuum. Direct proof of the realization of such a mechanism was obtained by the Chalmers group.<sup>100,101</sup> They did an experimental and theoretical study of the photodesorption of H<sub>2</sub>, HD, and D<sub>2</sub> from the terraced Cu(510) surface under the influence of blackbody radiation. The desorption is significant, since only a few bound states are contained in the shallow physisorption well, the vibrational motion of a molecule is dipole-active, and the dipole moment of the molecule–surface bond is a highly nonlinear function of the displacement.<sup>102</sup> The calculations showed that the rate of desorption initiated by an indirect process involving the excitation of phonons in the substrate is several orders of magnitude lower than that observed in experiment and calculated for the direct photodesorption mechanism.

Using the HREELS method, the authors of Refs. 100 and 101 had the capability of observing separately the photodesorption of molecules adsorbed on the flat terraces and on the edges of the steps. It was shown that the process of desorption from the steps is considerably more intense than from the terraces, and an isotope effect is also observed: deuterium is desorbed at a lower rate than hydrogen. The existence of such an isotope effect is explained by the theory. Without going into the details of the theory, we can posit that the deeper position of the level of zero-point vibrations of the D<sub>2</sub> molecule in the physisorption potential well in itself has an effect on the photodesorption rate. The differences in the rates of photodesorption from the terraces and edges of the steps is partly explained by the larger dipole activity of H<sub>2</sub> edge molecules, but additional study is required.<sup>101</sup>

## 4. OXYGEN, CARBON MONOXIDE, AND NITROGEN

### 4.1. Oxygen

The study of the low-temperature adsorption of oxygen on metals is of significant interest for at least two reasons. First, in interacting with a surface, oxygen, the most active component of the Earth's atmosphere, radically alters the properties of the surface (the electronic properties, catalytic reactions, corrosion, etc.), and the key stage of this interaction is adsorption. As in the case of hydrogen, the mechanism of dissociative adsorption may be a multistep one and might involve a precursor state—a state of physisorption. This state is characterized by a very small binding energy

(although larger for oxygen than for hydrogen), and deep cooling of the substrate is necessary in order to study it experimentally. Second, the formation of an adsorbed monolayer is the initial stage in the growth of an oxygen crystal, and the properties of this adlayer undoubtedly influence the properties of the cryocrystal that will grow.

The low-temperature adsorption of oxygen has been the subject of considerably fewer papers than hydrogen adsorption. Therefore, this Section of the paper is substantially shorter in length. We shall mainly discuss the low-temperature adsorption of oxygen on transition metals.

#### 4.1.1. Adsorption on metal films

The earliest study known to the author on the adsorption of oxygen under deep cooling of the substrate was done by Rühl,<sup>103</sup> who studied adsorption on as-deposited films of Mg, Mn, Al, In, Ga, Cd, Pb, and Sn with thicknesses of 50–150 Å, cooled to as low as 1.5 K. It was found that the adsorption (condensation) of oxygen at low temperatures (from 1.5 to 7 K for the different metals) does not have a substantial effect on the electrical resistivity of the film. However, increasing the temperature of the film to some characteristic temperature (e.g., in the range 20–40 K for Pb) leads to an irreversible increase in the resistance, which can be explained as being the start of an oxidation process which leads to an effective thinning of the film. Thus at low temperature oxygen is not chemisorbed on the surface of films of these metals but forms a layer of physisorbed or condensed molecular oxygen.

Similar results we later obtained by Chottiner and Glover<sup>104</sup> for tin films. Those authors point out<sup>104</sup> that in the condensation of a thick layer of oxygen at 5 K the resistance of the film increased somewhat, corresponding to the loss of metallic conduction by a layer with an effective thickness of 0.1 Å (their Sn film had a thickness of ~150 Å). Increasing the temperature of the film above 13 K led to an irreversible increase in the resistance owing to the chemisorption of oxygen. The authors of Ref. 104 estimated that this increase in resistance corresponds to eliminating a layer of tin ~11 Å thick from participation in the electrical conduction, and the activation energy of the chemisorption process is ~35 meV. A slight increase in the resistance of the film at 5 K can be explained as being due a change in the conditions of scattering of conduction electrons on the Sn–O<sub>2</sub> interface, since in the case of physisorption there is practically no exchange of electrons between the adsorbent and adsorbate.

#### 4.1.2. Adsorption on single crystals

*4.1.2.1. Spectra of adsorption states.* The adsorption of oxygen on single-crystal tungsten (the (110) face) at 20 K was first studied by Leung and Gomer,<sup>105</sup> who measured the thermodesorption spectra for the first time. They showed that at a relatively low exposure the thermodesorption spectrum of an adlayer formed at 20 K does not differ from that observed after adsorption at 300 K, and oxygen is desorbed predominantly in the form of atoms. The desorption of atomic oxygen after adsorption at room temperature has also been observed in our studies.<sup>40,41,106</sup> With increasing exposure to oxygen at 20 K the authors of Ref. 105 observed the

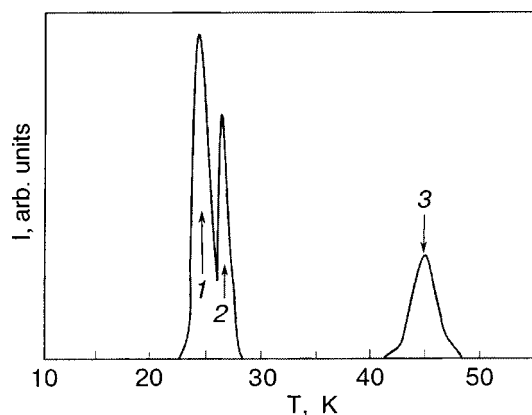


FIG. 27. Thermodesorption spectrum for oxygen from W(110); adsorption at 20 K.<sup>105</sup> 1—Condensation; 2—physisorption; 3—weak molecular chemisorption.

appearance of low-temperature peaks at 45 K, then at 27 K, and, finally, at 25 K. The corresponding adsorption states will be referred to by the temperature of the peaks. A thermodesorption spectrum of this type is shown in Fig. 27. The peaks at 45 and 27 K saturate with increasing exposure, while the peak at 25 K grows without bound. On the basis of measurements of the work function and electron-stimulated desorption, the authors of Ref. 105 concluded that the 27 and 25 K adsorption states are almost identical in their properties and pertain to physisorption and condensation, respectively. The 45 K adsorption state was attributed in Ref. 105 to a state of weak molecular chemisorption, and it was assumed that it is populated via conversion from a state of physisorption as the temperature is raised. A similar point of view is also expressed in the paper by Wang and Gomer,<sup>107</sup> but this interpretation was later acknowledged by Gomer *et al.*<sup>108</sup> to be incorrect.

To elucidate the nature of the adsorbed particles (atoms or molecules) on W(110) at  $T_s \sim 20$  K, an experiment was done using the oxygen isotopes  $^{16}\text{O}_2$  and  $^{18}\text{O}_2$ , and the desorption was observed at 45 K.<sup>108</sup> The idea of the experiment was as follows. If  $^{18}\text{O}_2$  and then  $^{16}\text{O}_2$  are adsorbed in sequence, then under the condition that all of the oxygen is adsorbed in a molecular state, the number of  $^{18}\text{O}_2$  and  $^{16}\text{O}_2$  molecules desorbed at 45 K will be in the same ratio as the number of these molecules adsorbed. The experiment showed, however, that only desorption of  $^{16}\text{O}_2$  is observed at 45 K. This means that the first portion of the molecules ( $^{18}\text{O}_2$ ) dissociated, and the desorption of chemisorbed oxygen atoms occurs at  $T > 2000$  K. However, the authors of Ref. 108 note that in the given experimental setup one cannot rule out that the atomic phase of adsorption was formed not directly during adsorption but as a result of conversion when the sample temperature was raised to bring about thermodesorption. That that was in fact not the case is shown by the experiments of Opila and Gomer using photoelectron spectroscopy,<sup>109</sup> which we shall discuss below.

The above-described state of the adsorbed oxygen is typical for tungsten, but in the case of platinum Artsyukovich and Ukraintsev<sup>110</sup> observed the conversion of  $\text{O}_2$  molecules physisorbed at  $T_s \sim 20$  K to a chemisorbed state when the temperature  $T_s$  was raised to 30–40 K. An atomic chemisorbed state is observed when  $T_s$  is increased to 100–160 K.

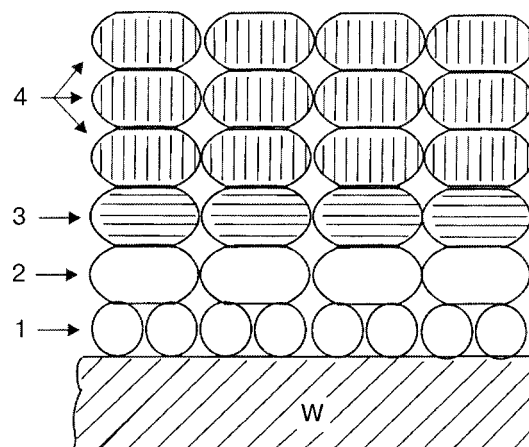
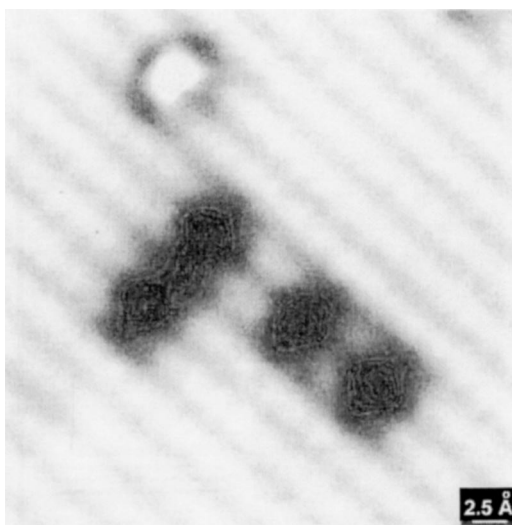


FIG. 28. Model of an oxygen adlayer at  $T_s \sim 5$  K.<sup>34</sup> 1—Atomic chemisorption; 2—molecular chemisorption; 3—physisorption; 4—condensation.

We have measured the thermodesorption spectrum of oxygen adsorbed at  $T_s \sim 5$  K on different faces of tungsten.<sup>33,34,111</sup> The thermodesorption spectra of molecular oxygen from the W(110), (100) and (112) surfaces<sup>33,34</sup> are similar to each other and are practically the same as the spectrum obtained for W(110) by Leung and Gomer.<sup>105</sup> What is new here is evidence of the absence of oxygen adsorption states on the tungsten surface with a binding energy less than that for the 25 K state. The spectrum of thermodesorption of oxygen from the W(111) surface is somewhat different from the spectra discussed above for the W(110), (100) and (112) faces. The difference is that the peak corresponding to weak molecular chemisorption is shifted to 60 K.<sup>111</sup> An estimate of the activation energy for desorption for the 25, 27, 45, and 60 K adsorption states gives 65, 70, 117, and 156 meV, respectively. We see the cause of the increase in the binding energy of  $\text{O}_2$  in the state of weak molecular chemisorption on the (111) face as being that this face is the least densely packed, and molecules on this face can touch a larger number of neighboring W atoms than in the case of the smoother faces. Based on the results discussed above, a hypothetical model for the layer-by-layer growth of an oxygen cryocrystal was proposed in Ref. 34 and is illustrated in Fig. 28.

Let us conclude by discussing the results of direct observations by the method of scanning tunneling microscopy of the oxygen atoms and molecules on the surface of a metal cooled to 4 K.<sup>112</sup> The authors of Ref. 112 observed individual  $\text{O}_2$  molecules, clusters of  $\text{O}_2$  molecules, and also oxygen atoms adsorbed on the Cu(110) surface at  $T_s \sim 4$  K. Figure 29 shows an STM image of a  $37 \times 37$  Å region of the surface, on which one can see an oxygen molecule (the bright spot) and pairs of oxygen atoms (dark spots). The authors of Ref. 112 see these results as proof that a molecular precursor state actually exists on the surface and participates in the mechanism of dissociative adsorption, although some recent papers have cast doubt on the role of the precursor state.<sup>50–53</sup> The important fact is that molecules are present on a surface on which dissociative adsorption occurs.

**4.1.2.2. Adsorption kinetics.** Let us consider the curves measured in our laboratory by the molecular-beam method (Sec. 2.5) for the dependence of the oxygen sticking coeffi-

FIG. 29. STM image of oxygen adparticles on Cu(110) at 4 K.<sup>112</sup>

cient on the degree of coverage  $\theta$  for different faces of W.<sup>33,34,111,113,114</sup>

Figure 30, taken from Ref. 34, shows the dependence of the sticking coefficient on  $\theta$  for different substrate temperatures  $T_s$  for the (100) and (110) faces of tungsten. We note that here and below,  $\theta$  is the number of oxygen atoms per atom of the substrate surface. In the case of the W(100) surface the  $S(\theta)$  curves are characterized by the following features. The initial sticking coefficient is independent of  $T_s$

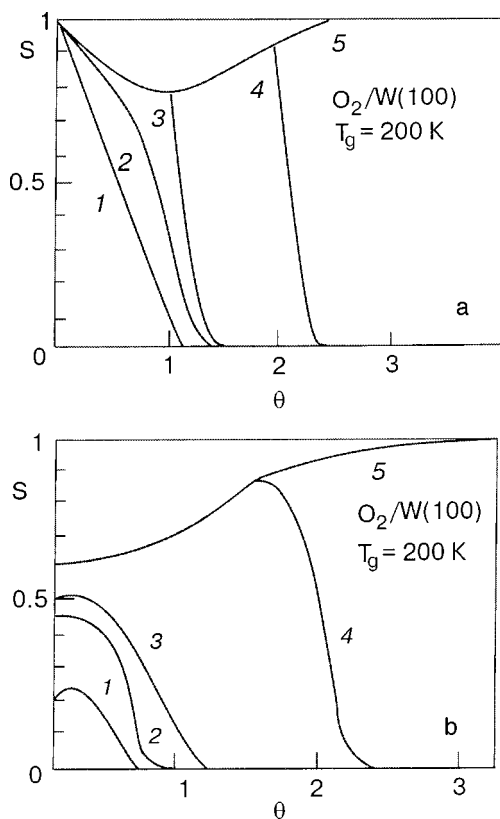


FIG. 30. Sticking coefficient for  $O_2$  versus the degree of coverage.<sup>34</sup> a) W(100),  $T_s$  [K]: 340 (1), 200 (2), 80 (3), 35 (4), 5 (5); b) W(110),  $T_s$  [K]: 300 (1), 80 (2), 60 (3), 35 (4), 5 (5).

and equal to unity. The initial sticking coefficient is also independent of  $T_g$ . This attests to direct, nonactivated chemisorption.

In the previous paragraph we presented evidence that oxygen is dissociatively chemisorbed in the form of atoms on tungsten up to a certain coverage at  $T_s > 20$  K. It seems to us that the results presented in Fig. 30 attest to the fact that dissociative adsorption of oxygen also occurs at 5 K. It is seen that curves 4 and 5 in Fig. 30 coincide at coverages up to one monolayer. That means that in this coverage range the mechanism of adsorption is unchanged on going from  $T_s \approx 35$  K to  $T_s \approx 5$  K, i.e., the adsorption is dissociative at  $T_s \approx 5$  K also.

Let us now discuss the influence of the substrate temperature in the range 5–350 K on the kinetics of filling of the first monolayer. Such data have been obtained for  $T_g = 200$  K. It is seen in Fig. 30 that for  $T_s \approx 350$  K the sticking coefficient decreases sharply with coverage, attesting to a Langmuir mechanism of adsorption, wherein a molecule incident on an occupied adsorption center is reflected back. Lowering  $T_s$  leads to a decrease in the slope of the  $S(\theta)$  curve, which indicates the turning on of a mechanism of adsorption via an extrinsic precursor state, when a molecule incident on an occupied center migrates along the surface and may find an unoccupied center and be adsorbed. Some qualitative ideas as to the cause of the increased role of adsorption via an extrinsic precursor state as  $T_s$  is lowered can be found in our review article;<sup>11</sup> these ideas are based on a comparison of the lifetime of a molecule on the surface in respect to the thermodesorption process,  $\tau$ , and the time required for traversing a certain diffusion path,  $t_m$ . Since the activation energy for desorption,  $E_d$ , is always larger than the activation energy for surface diffusion,  $E_m$ , with decreasing temperature the balance of these times changes in favor of diffusion:

$$\frac{\tau}{t_m} \approx \exp\left(\frac{E_d - E_m}{kT_s}\right). \quad (4.1)$$

The next feature of the curves shown in Fig. 30 is that after completion of the first monolayer the sticking coefficient increases, approaching unity. This effect, as in the adsorption of hydrogen (paragraph 3.1.2.1), is explained by the increase in the efficiency of kinetic energy loss in the collision of a molecule with the surface as the surface fills with the weakly bound molecular adsorption phase on account of the equal mass of the colliding partners.

The kinetic energy of the incident molecules, while not affecting the initial sticking coefficient, nevertheless has a substantial influence on the sticking coefficient in the region  $\theta \approx 1$ , where the formation of the molecular adsorption phase begins. The sticking coefficient at  $\theta \approx 1$  decreases with increasing  $T_g$  as a result of the decrease in the probability of trapping to a state of physisorption. A qualitatively similar influence of the energy of the incident particles on the sticking probability has been observed, e.g., for nitrogen on W(100) (Ref. 115) and CO and Ar on Ir(110) (Ref. 116) (granted, at significantly higher  $T_s$ ).

The adsorption of oxygen on the W(112) surface at  $T_s \sim 5$  K is characterized by  $S(\theta)$  curves like those shown in Fig. 30,<sup>34</sup> except for substantial differences in the case of

adsorption on the close-packed W(110) surface. As is seen in Fig. 30, the initial sticking coefficient for W(110) is substantially less than unity and it decreases with increasing  $T_s$ . The reason why  $S_0$  is substantially less on the W(110) surface may be discerned in the fact that the number of broken bonds per unit area on this surface is 1.4 times less than on the W(100) surface.

The decrease of  $S_0$  with increasing  $T_s$  is a sign of participation of an intrinsic precursor state in the dissociative adsorption mechanism (arguments toward a similar conclusion are given in paragraph 3.1.1.1). In contrast to W(100) and W(112), in the case W(110) the signs of adsorption via an extrinsic precursor state are manifested at room temperature. This can be explained by the higher mobility of the  $O_2$  molecules in the precursor state on the close-packed, smooth W(110) surface. The increase in the sticking coefficient on the W(110) surface for  $\theta > 1$  is similar to the W(100) case and is explained by the same cause.

We know of no studies in which  $S(\theta)$  has been measured for adsorption on a metal at  $T_s \sim 5$  K. However, Wang and Gomer<sup>117</sup> have obtained similar curves for W(110) at  $T_s \geq 20$  K. In their general features these curves for  $T_s \sim 20$  K are similar to that shown in Fig. 30: the values of the initial sticking coefficients are close, and one observes an increase in the sticking coefficient with increasing coverage. However, according to our measurements, the increase of  $S$  with increasing  $\theta$  does not become noticeable at zero coverage, as in Ref. 117, but for  $\theta > 0.5$ . The authors of Ref. 117 also attribute the increase of  $S$  with increasing  $\theta$  to more efficient kinetic energy loss by the incident molecule in its impact on a previously adsorbed molecule. What is hard to explain is the finding of Ref. 117 that  $S$  increases starting at zero coverage, when, according to our data and the data of Gomer *et al.*,<sup>107,108</sup> tightly bound chemisorbed oxygen atoms accumulate on the surface. The O–W complex is essentially a unified quasimolecule with a very large mass, and the collision of an  $O_2$  molecule with it is characterized by inefficient accommodation.

**4.1.2.3. Electron spectroscopy and the state of adsorbed particles.** Let us discuss the results of several studies using photoelectron spectroscopy to elucidate the state of adsorbed particles at low temperatures and also a study using x-ray absorption-edge fine structure (NEXAFS) for the same purpose. We have already mentioned the paper by Opila and Gomer,<sup>109</sup> in which the adsorption of oxygen on W(110) at  $T_s = 26$  K was studied by the methods of ultraviolet (UPS) and x-ray (XPS) photoelectron spectroscopy. It was found that from the start of the oxygen admission only atomic chemisorbed oxygen is formed, and only after saturation of the atomic layer does a layer of weakly bound molecular oxygen begin to grow (and, with time, saturate). In the XPS spectrum one observes two main oxygen peaks, one of which (530.5 eV) belongs to atomic oxygen and does not undergo any changes (Fig. 31), unlike the 536 eV peak, which vanishes from the spectrum after the substrate is heated to 90 K (the molecular phase is desorbed). Based on the fact that for the molecular phase a single unsplit peak is observed in the XPS spectrum, the assumption was made in Ref. 109 that both atoms of the  $O_2$  molecule are found in an identical

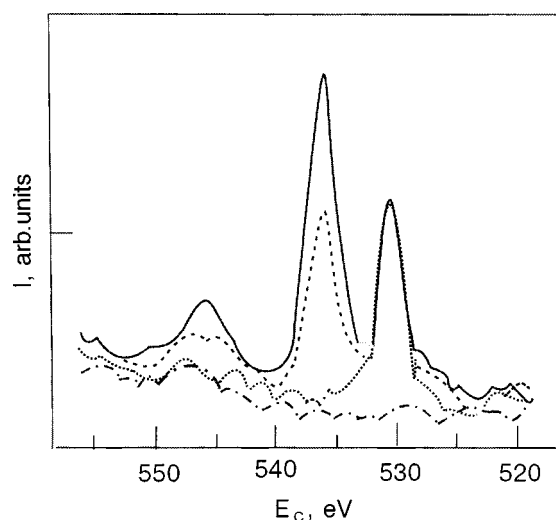


FIG. 31. Photoelectron spectrum of adsorbed oxygen.<sup>109</sup> The solid curve is for a saturated layer at 26 K; the dashed curve—heated to 36 K; the dotted curve—heated to 90 K; the dot-and-dash curve—clean W.

position with respect to the substrate, i.e., the axis of the molecule is oriented parallel to the surface.

We know of several more studies in which the method of photoelectron spectroscopy was used to elucidate the state of oxygen adsorbed on a metal surface at low temperatures. Schmeisser and Jacobi<sup>118</sup> did a UPS study of the adsorption of oxygen on the surface of sputtered gallium films. It was found that at 10 K the oxygen molecules are physisorbed in the first monolayer, and above it several additional  $O_2$  monolayers can be condensed. When  $T_s$  is increased to 70 K the  $O_2$  molecules are chemisorbed (without dissociation), and at 300 K the oxygen is bound dissociatively and forms a bulk oxide.

The UPS method was used by Jacobi *et al.*<sup>119</sup> in a study of the adsorption of oxygen on the Ni(100) surface ( $T_s = 20$  K). The authors of Ref. 119 showed that at submonolayer coverages, oxygen is adsorbed mainly dissociatively, although physisorbed molecules are also noticeable. With increasing exposure a layer of physisorbed molecules is formed exclusively atop the chemisorbed monolayer. Thus on the Ni(100) surface the low-temperature adsorption of oxygen occurs in a manner similar to that on the W surface (see above).

A study of oxygen adsorption at  $T_s = 25$  K on the Pt(111) surface has been done by Lunz *et al.*<sup>120</sup> with the use of XPS and TPD. The photoelectron and thermodesorption spectra reveal four different states of the adsorbed particles: poly-layer condensation (desorption temperature  $T_d = 30$  K), physical adsorption ( $T_d = 45$  K), and molecular chemisorption ( $T_d = 750$  K). The physisorption serves as a precursor state for molecular chemisorption, and the latter, in turn, is a precursor state for atomic chemisorption. The position of the  $O1s$  peak in the spectrum of physisorbed oxygen is close to that for the gas phase.

The same adsorption system  $O_2$ /Pt(111) was studied by Ranke<sup>121</sup> by the methods of XPS and UPS. In that paper it was also shown that at 20 K oxygen is physisorbed in molecular form. As a result of a heating of the substrate to 90 K the photoelectron spectrum is transformed, attesting to mo-

molecular chemisorption in the form of  $O_2^-$  or  $O_2^{2-}$  (the superoxo and peroxy configurations, respectively). Such states of the oxygen molecules adsorbed on platinum have been identified by calculations from first principles in the local-spin-density approximation.<sup>122</sup> In their general features the results of Ref. 121 agree with those obtained by the TPD method in Ref. 110.

High-resolution electron-energy loss spectroscopy (HREELS) has been used to study the states of adsorbed oxygen at  $T_s \leq 20$  K on the surfaces Ni(111) (Ref. 123) and Nb(110) (Ref. 124). This variety of electron spectroscopy is extremely efficient for identifying physisorbed molecules from the corresponding characteristics of energy loss to the excitation of intermolecular vibrations. In the study by Beckerle *et al.*<sup>123</sup> an attempt was made to observe  $O_2$  molecules in a precursor state at  $T_s = 8$  K in the limit of zero coverage. However, this attempt was not successful, apparently because of the very short lifetime of molecules in the precursor state and their very low density.

Franchy *et al.*<sup>124</sup> established that at  $T_s = 20$  K at low exposures the oxygen on the Nb(110) surface is chemisorbed dissociatively, a circumstance that the authors associate with the formation of the oxide NbO. At high exposures a physisorbed molecular layer forms above the chemisorbed atomic monolayer, much like what happens on the surface of tungsten (see above).

The HREELS method has also been used for studying the resonance scattering of electrons by an oxygen layer physisorbed on the surface of silver in the studies of Tang *et al.*<sup>125</sup> and Lacombe *et al.*<sup>126</sup> In particular, in Ref. 126 it is shown that the angular dependence of the scattered electrons changes at the transition from monolayer coverage to multilayer coverage; this is a consequence of the different orientation of the molecules in the monolayer and multilayer regimes.

Still another variety of electron spectroscopy—transmission spectroscopy—was used by Shayegan *et al.*<sup>127</sup> to study the state of the adparticles in the adsorption of oxygen on the Ni(111) surface at  $T_s = 5.5$  K. In measuring the current–voltage characteristic in a retarding field in the saturation region one observes current oscillations characterizing the state of the adsorbed layer.<sup>128</sup> The form of the spectrum obtained in Ref. 127 indicates that the  $O_2$  molecules are physisorbed on the surface. Heating of the sample leads to the formation of a chemisorption state; the activation energy of this process is  $\sim 13$  meV. At first glance the results of the studies of low-temperature adsorption of oxygen on nickel in Refs. 127 and 119 are contradictory: in Ref. 119 the dissociative chemisorption of oxygen was observed. It should be taken into consideration, however, that different faces of single-crystal nickel were investigated in Refs. 127 and 119, and, furthermore, the temperature of the sample in Ref. 119 was substantially higher than in Ref. 127 (20 K rather than 5.5 K). It is quite possible that a temperature of 20 K is sufficient for overcoming the insignificant activation barrier between the states of physisorption and chemisorption.

Important information about the state of adsorbed oxygen can be obtained by the NEXAFS method. Such experiments done in synchrotron radiation for the adsorption system  $O_2/Pt(111)$  at  $T_s = 17$  K are described by Wurth *et al.*<sup>129</sup>

At a substrate temperature  $T_s < 30$  the NEXAFS spectrum and, accordingly, the intramolecular structure of the adsorbed oxygen are almost indistinguishable from the van der Waals-bound solid oxygen, and this is a state of physical adsorption with van der Waals bonding. When the substrate temperature is raised to 80 K conversion to a chemisorbed molecular state is observed, as is attested by the transformation of the NEXAFS spectrum. Because of the involvement of the  $\pi^*$  orbital perpendicular to the surface in the chemisorption bond, the corresponding resonance is weak and broadened, while the  $\pi^*$  orbital parallel to the surface remains unperturbed. The results indicate that in both the physisorption and chemisorption states the axis of the  $O_2$  molecule is oriented parallel to the surface. The transition to the state of chemisorption also leads to a change in the magnetic properties of the  $O_2$  molecule, which is manifested in exchange splitting of the  $\sigma^*$  resonance. Thus in the case of the low-temperature adsorption of oxygen on platinum, dissociation of the  $O_2$  molecule does not occur, as it does in the case of adsorption on tungsten.

*4.1.2.4. Adsorption of oxygen and scattering of conduction electrons.* Panchenko and co-workers used the static skin-effect method not only to study the low-temperature adsorption of hydrogen (Sec. 3.1.3) but also to study the adsorption of oxygen.<sup>23,25,75,76,130</sup> It was shown<sup>23</sup> that the resistivity of thin ( $\sim 0.1$  mm) single-crystal slabs of tungsten and molybdenum with (110) surfaces in a strong magnetic field parallel to the surface is anomalously sensitive to the adsorption of oxygen. The deposition of a disordered monolayer of oxygen leads to a twofold increase in the magnetoresistance. In Refs. 75 and 76 it was established that the effect depends on the crystallographic orientation of the surface of the slab, and for a slab with the (100) surface the resistivity remains practically unchanged. An interpretation of this difference in the behavior of the resistivity of slabs with the (110) and (100) surfaces was proposed in Refs. 75 and 76, based on taking into account the electron–hole transfers in the scattering of conduction electrons by the surface.

The combined use of the static skin-effect and LEED methods in a single experimental apparatus<sup>25,130</sup> has permitted the establishment of a clear correlation between the resistance of the slab and the structure of the adsorbed oxygen layer, which is ordered by means of annealing. Figure 32, taken from Ref. 25, shows the dependence of the magnetoresistance of a tungsten slab with the (110) surface on the oxygen adsorption time; the vertical lines bound the existence intervals of the corresponding structures of the adlayer. It is seen that the sharp minimum of the magnetoresistance is achieved at the maximum development of the  $p(2 \times 1)$  structure, and upon the formation of the  $(2 \times 2)$  structure the magnetoresistance again increases. Analysis of the electronic transitions in scattering from the corresponding surface structures explains the specular character of the electron scattering for the  $p(2 \times 1)$  surface and the diffuse character of the scattering for  $(2 \times 2)$ .

A substantially different situation obtains for the adsorption of oxygen on the Mo(110) surface.<sup>131</sup> On that surface the  $p(2 \times 1)$  structure does not form, and therefore the dependence of the magnetoresistance on the oxygen adsorption time does not have a sharp minimum like that observed for

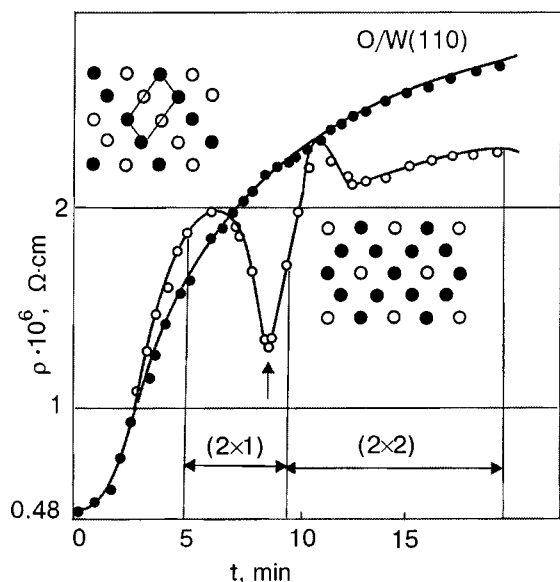


FIG. 32. Magneto-resistance of a W(110) slab versus the exposure time in oxygen.<sup>8,25</sup> ●—Adsorption at  $T_s=4.2$  K; ○—annealing to 200 K; the vertical lines are boundaries of the existence regions of the structures illustrated in the figure.

the W(110) surface. Thus, as in the case of hydrogen adsorption (Sec. 3.1.3), the static skin-effect method can serve as a nondestructive indicator of the structure of an oxygen adlayer.

## 4.2. Carbon monoxide and nitrogen

Study of the low-temperature adsorption of carbon monoxide and nitrogen is of interest from the standpoint of elucidating the mechanism of their adsorption and participation in important catalytic processes (in particular, in the role of an adsorption precursor state), e.g., the oxidation of CO in automobile exhaust or the synthesis of ammonia, and also as the initial stage of the growth of cryocrystals. We know of only a small number of papers devoted to the study of low-temperature adsorption of these gases, and so this Section will be extremely short.

### 4.2.1. Carbon monoxide

Let us briefly discuss a few of the papers known to us on the low-temperature adsorption of carbon monoxide. Leung, Vass, and Gomer<sup>132</sup> have studied the influence of CO adsorption on the W(110) surface at  $T_s=20$  K on the work function and electron-stimulated desorption. It was shown that the work function increases by 0.6 eV and that electron-stimulated desorption of  $\text{CO}^+$  ions from the adlayer occurs.

Norton *et al.*<sup>133</sup> have studied the adsorption of CO on the surface of the noble metals copper and gold at  $T_s=20$  K by the method of photoelectron spectroscopy. The spectra of physisorbed CO exhibit only a slight broadening and shift of the  $5\sigma$ ,  $1\pi$ , and  $4\sigma$  levels in comparison with the gas phase. Heating of the substrate to 30 K leads to conversion of the physisorbed to a chemisorbed state, which indicates that this process has a very low activation energy.

The resonance scattering of electrons from a silver surface coated with a CO adlayer at 20 K has been investigated by Demuth *et al.*<sup>134</sup> It was found that the frequency of intermolecular vibrations differs little from that in the gas phase.

It was also shown that the differences in the electron spectra of the adsorbed and condensed phases of CO permit one to delimit the monolayer and multilayer deposition regimes.

The adsorption of CO on the Ni(100) surface at  $T_s=20$  K was studied by Jacobi *et al.*<sup>119</sup> by the UPS method. Those authors found that on this surface CO is chemisorbed in the first layer. This is evidence of a low activation energy for chemisorption. Information about the dependence of the sticking coefficient of CO on the coverage was also obtained, and it was stated that the sticking coefficient is constant up to a coverage of  $\theta=0.9$ .<sup>119</sup> This last result indicates that the mobility of the CO molecule is very high, and it can therefore easily find an unoccupied adsorption center (adsorption via an extrinsic precursor state).

Shayegan *et al.*<sup>135</sup> have used the method of transmission electron spectroscopy to study the adsorption of CO on the Ni(111) surface at  $T_s=5.5$  K. The suppression of the electron current in the saturation region of the current–voltage characteristic attests to the formation of a physisorbed layer.<sup>128</sup> The authors of Ref. 135 called attention to the fact that the physisorbed CO is present at  $T_s=5.5$  K even at submonolayer coverages. This conclusion contradicts the conclusions of Ref. 119, though it must be taken into consideration that in Ref. 119 the temperature was significantly higher. Furthermore, the Ni(100) surface studied in Ref. 119 is less densely packed than the Ni(111) surface investigated in Ref. 135, making it more favorable for the formation of a chemisorption bond.

Kawai and Yoshinobu have studied the low-temperature ( $T_s\sim 20$  K) adsorption of CO on the Pt(111) and Ni(100) surfaces by the method of infrared spectroscopy.<sup>136,137</sup> By comparing the intensity of the different peaks in the spectra, those authors<sup>136,137</sup> determined the relationship between the occupations of the adsorption sites (centers) of different kinds in different stages of the adsorption process and arrived at the conclusion that under conditions of suppressed surface migration of the CO molecules (because of the low  $T_s$ ) there occurs not only direct adsorption at energetically favorable sites but also stimulated occupation of neighboring adsorption sites in collisions of the incident molecules with previously adsorbed molecules.

In concluding our review of papers on the low-temperature adsorption of CO we point out the study by Sautet *et al.*,<sup>138</sup> who used the STM method at  $T_s=25$  K to observe individual CO molecules adsorbed at different kinds of sites on the Pd(111) surface. Figure 33 shows an STM image of individual CO molecules. The molecules are seen as protrusions of height  $\sim 0.25$  and  $\sim 0.15$  Å above the surface, which indicates that they are adsorbed at sites of two different types. This interpretation is confirmed by theoretical calculations of the total energy in the density-functional approximation.

### 4.2.2. Nitrogen

Research on the adsorption of nitrogen on metals surfaces at low temperatures ( $T_s\leq 20$  K) has been the subject of a small number of papers known to us.<sup>84,119,134,139–142</sup> These are mainly studies using methods of electron spectroscopy. Using the XPS method, Grunze *et al.*<sup>139</sup> observed a significant difference in the spectra of N(1s) for nitrogen chemi-



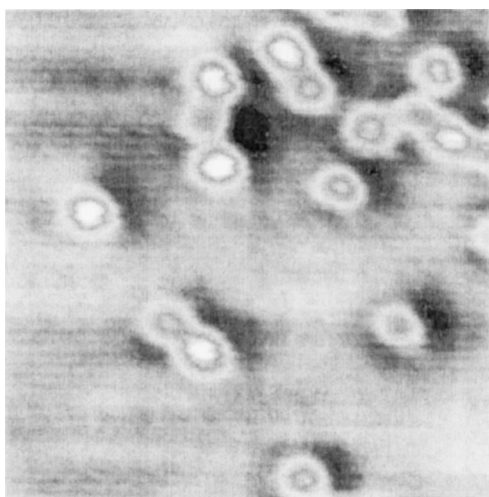


FIG. 33. STM image of CO on Pd(111) at 25 K.<sup>138</sup>

sorbed and physisorbed on the Ni(100), Re(0001), and W(100) surfaces, while the spectra of physisorbed and gas-phase nitrogen are similar. An attempt to detect the nitrogen molecule in an intrinsic precursor state above the clean surface was unsuccessful, most likely because of the very fast conversion of the N<sub>2</sub> molecule from an intrinsic precursor state to a state of chemisorption. If that is the case, then the activation barrier for the transition to a state of chemisorption is very low ( $\leq 30$  meV).

Jacobi *et al.*<sup>119</sup> used an angle-resolved UPS method to study the adsorption of nitrogen on the Ni(100) surface at  $T_s = 20$  K. At submonolayer coverages they detected mainly chemisorbed N<sub>2</sub> molecules, although there was an “impurity” of physisorbed molecules. With increasing exposure a layer of physisorbed molecules was formed. The positions of the peaks of the valence levels were shifted by an amount equal to the change in work function due to the adsorption of the first monolayer. From the fact that chemisorption is present at 20 K, as in Ref. 139, Jacobi *et al.*<sup>119</sup> concluded that the activation energy for chemisorption of N<sub>2</sub> on Ni(100) is very small.

Schmeisser *et al.*<sup>140</sup> used the UPS method to study the adsorption of nitrogen on the surface of nickel films at  $T_s = 7$  K. The photoelectron spectrum shows the characteristic signs of physisorbed N<sub>2</sub> molecules. From the relative intensities of the peaks of the  $4\sigma$ ,  $1\pi$ , and  $5\sigma$  levels and the weakly expressed splitting of the  $1\pi$  level, those authors concluded that the molecules are oriented not randomly, as in a gas, but with their axes parallel to the surface.

In several studies the adsorption of nitrogen on the surface of silver has been studied at low  $T_s$  by methods of electron spectroscopy. Gruyters and Jacobi<sup>84</sup> observed inhomogeneous inelastic scattering of electrons on the Ag(111) surface owing to excitation of vibrational and rotational modes in physisorbed nitrogen molecules. The overlap of the vibrational and rotational modes in the case of nitrogen leads to the formation of structureless inelastic tails of the stretching vibrations and their overtones. The coadsorption of nitrogen and hydrogen was also studied.

As in Ref. 84, Demuth *et al.*<sup>134</sup> studied the resonance inelastic scattering of electrons from a layer of nitrogen mol-

ecules physisorbed on the surface of a silver film. This scattering is due to the formation of a short-lived state of the negative ion (lifetime  $\leq 10^{-14}$  s). An incident electron of resonant energy is trapped, and after the decay of this state the N<sub>2</sub> molecule is left vibrationally excited. The vibrational frequency differs insignificantly from that for the gas phase. Slight differences in the excitation spectrum allow one to distinguish an adsorbed monolayer from a condensed multilayer.

Bartolucci and Franchy<sup>141</sup> used the HREELS, TDS, and LEED methods to study the adsorption of nitrogen on the Ag(110) surface at  $T_s = 15$  K. They observed an ordered structure matched with the substrate in the first monolayer and an unmatched hexagonal structure in the condensed multilayer. For the multilayer they observed a resonance inelasticity scattering of electrons involving the excitation of the N–N bond with the participation of a short-lived state of the negative ion.

Jacobi *et al.*<sup>142</sup> studied the resonance negative-ion scattering of electrons from an N<sub>2</sub> monolayer adsorbed at  $T_s = 20$  K on the Al(111) surface. The stretching vibrations were excited by resonance scattering of electrons with the formation of a short-lived state of the negative ion. In addition, the authors of Ref. 142 observed suppression of the mode of stretching vibrations of N<sub>2</sub> upon the coadsorption of 0.16 monolayer of water. This effect was attributed to quenching of the negative-ion resonance of the N<sub>2</sub> molecules by the water.

## 5. CONCLUSION

The main feature of the low-temperature adsorption of gases is the formation and steady maintenance of a physisorbed layer of molecules (for transition metals this occurs after the formation of a chemisorbed adlayer, while for noble metals it occurs right from the start). This makes it possible to study the properties of the physisorbed layer and the mechanisms of its formation.

The most diverse and interesting effects have been observed for the adsorption of hydrogen. The difference of the quantum properties (the levels of zero-point vibrations) of the H<sub>2</sub> and D<sub>2</sub> molecules give rise to various isotope effects, particularly in the kinetics of adsorption–desorption processes on surfaces of W and Mo. This, in turn, is due to the very high mobility of the H<sub>2</sub> molecules and the possibility of formation of clusters or islands of the 2D condensate. It is possible that the anomalously high mobility of the H<sub>2</sub> molecules is the cause of a “catastrophic” drop in the sticking probability at coverages where the formation of an atomic adsorption phase on Mo(110) is completed. We do not rule out the possibility that quantum tunneling diffusion is involved in this process, and to check this the substrate temperature should be lowered to  $\leq 3$  K. The strong isotope effect in the electron-stimulated disordering of the adlayer is also worthy of note. Study of the adsorption kinetics has yielded considerable information about the role of the precursor state and the character of the molecule–surface interaction potential.

Much valuable information has been obtained in the study of hydrogen adsorption on the surfaces of noble metals with the use of monoenergetic molecular beams and the

methods of electron spectroscopy. It has been established that the vibrational–rotational properties of physisorbed molecules are similar to the properties of the molecules in the gas phase. It was concluded from the experiments and theoretical calculations that the classical model is inadequate, and it is necessary to employ a quantum model of sticking which takes into account the inelastic interaction of the molecules with the surface with excitation of phonons. Subtle mechanisms of sticking with the participation of trapping of the molecule in a quasibound adsorption state in the resonance excitation of rotational states and diffraction on the lattice of surface atoms have been revealed. Substantial differences in ortho–para conversion on flat and terraced faces of single crystals have been found. The amortization effect, which leads to an increase in the sticking coefficient with coverage, is interesting.

Research results on the low-temperature adsorption of oxygen and, especially, carbon monoxide and nitrogen are much more scarce. For oxygen the set of adsorption states realized at  $T_s \geq 5$  K has been determined. On transition metals these states are, in order of increasing surface density, atomic chemisorption, weak molecular chemisorption, physisorption, and condensation. The initial stage of growth of an oxygen cryocrystal looks the same. For studying the adsorption of  $O_2$ ,  $CO$ , and  $N_2$  the method of photoelectron spectroscopy is often used, and the state of the adparticles (chemisorption or physisorption) and the orientation of the molecules relative to the surface have been determined. Isolated attempts to observe atoms and molecules adsorbed at low temperature by STM should also be mentioned.

So, has it been worth it to “break the bank” in struggling with the difficulties of adsorption experimentation at low temperatures? This is for the reader to judge, but the author wishes to answer in the affirmative. Without lowering the temperature of the sample one could not observe the many subtle and beautiful effects that enrich our understanding of the mechanism of adsorption phenomena. We think it advisable to do research at still lower temperatures, especially for hydrogen.

The author is sincerely grateful to N. V. Petrova and V. S. Manzhara for assistance in preparing the manuscript.

\*E-mail: ptush@iop.kiev.ua

<sup>1</sup>K. Christmann, *Surf. Sci. Rep.* **9**, 1 (1988).

<sup>2</sup>C. R. Arumainayagam and R. J. Madix, *Prog. Surf. Sci.* **38**, 1 (1991).

<sup>3</sup>K. D. Rendulic, *Surf. Sci.* **272**, 34 (1992).

<sup>4</sup>A. Gross, *Surf. Sci. Rep.* **32**, 291 (1998).

<sup>5</sup>G. J. Kroes, *Prog. Surf. Sci.* **60**, 1 (1999).

<sup>6</sup>É. Zenguil, *Surface Physics* [Russian translation], Part 2, Mir, Moscow (1990).

<sup>7</sup>E. Ilisca, *Prog. Surf. Sci.* **41**, 217 (1992).

<sup>8</sup>O. A. Panchenko, P. P. Lutsishin, and S. V. Sologub, *Prog. Surf. Sci.* **69**, 193 (2002).

<sup>9</sup>A. G. Naumovets, *Fiz. Nizk. Temp.* **20**, 1091 (1994) [*Low Temp. Phys.* **20**, 857 (1994)].

<sup>10</sup>E. Pijper, M. F. Somers, G. J. Kroes, R. A. Olsen, E. J. Baerends, H. F. Busnengo, A. Salin, and D. Lemoine, *Chem. Phys. Lett.* **347**, 277 (2001).

<sup>11</sup>Yu. G. Ptushinskii and B. A. Chuikov, *Poverkhnost'. Fiz. Khim. Mekh.*, No. 9, 5 (1992).

<sup>12</sup>P. Kisliuk, *J. Phys. Chem. Solids* **3**, 95 (1957).

<sup>13</sup>J. Harris and S. Andersson, *Phys. Rev. Lett.* **55**, 1583 (1985).

<sup>14</sup>M. I. Elinson and G. F. Vasil'ev, *Field Emission* [in Russian], Gos. Izd-vo Fiz. Mat. Lit., Moscow (1958).

<sup>15</sup>L. N. Dobretsov and M. V. Gomoyunova, *Emission Electronics* [in Russian], Nauka, Moscow (1966).

<sup>16</sup>R. Gomer, R. Wortman, and R. Lundy, *J. Chem. Phys.* **26**, 1147 (1957).

<sup>17</sup>V. K. Medvedev and A. O. Snitko, *Zh. Tekh. Fiz.* **57**, 1638 (1987).

<sup>18</sup>G. Mazenko, J. R. Banavar, and R. Gomer, *Surf. Sci.* **107**, 459 (1981).

<sup>19</sup>R. S. Polizotti and G. Ehrlich, *J. Chem. Phys.* **71**, 259 (1979).

<sup>20</sup>I. F. Lyuksyutov and A. G. Fedorus, *Zh. Éksp. Teor. Fiz.* **80**, 2511 (1981) [*Sov. Phys. JETP* **53**, 1317 (1981)].

<sup>21</sup>V. V. Gonchar, O. V. Kanash, I. A. Kotlyarova, A. G. Fedorus, and A. F. Fedosenko, *Zh. Éksp. Teor. Fiz.* **95**, 1773 (1989) [*Sov. Phys. JETP* **68**, 1023 (1989)].

<sup>22</sup>M. Strongin, J. M. Dickey, H. H. Farrell, T. F. Arns, and G. Hrabak, *Rev. Sci. Instrum.* **42**, 311 (1971).

<sup>23</sup>O. A. Panchenko, P. P. Lutsishin, and Yu. G. Ptushinskii, *Zh. Éksp. Teor. Fiz.* **66**, 2191 (1974) [*Sov. Phys. JETP* **39**, 1079 (1974)].

<sup>24</sup>V. F. Koval, P. P. Lutsishin, O. A. Panchenko, and S. V. Sologub, *Surf. Sci.* **331–333**, 1317 (1995).

<sup>25</sup>P. P. Lutsishin, T. N. Nakhodkin, O. A. Panchenko, and Yu. G. Ptushinskii, *Zh. Éksp. Teor. Fiz.* **82**, 1306 (1982) [*Sov. Phys. JETP* **55**, 759 (1982)].

<sup>26</sup>V. T. Cherepin and M. A. Vasil'ev, *Methods and Devices for Analysis of the Surface of Materials* [in Russian], Naukova Dumka, Kiev (1982).

<sup>27</sup>Ph. Avouris, D. Schmeisser, and J. E. Demuth, *Phys. Rev. Lett.* **48**, 199 (1982).

<sup>28</sup>S. Andersson and J. Harris, *Phys. Rev. Lett.* **48**, 545 (1982).

<sup>29</sup>É. Zenguil, *Surface Physics* [Russian translation], Mir, Moscow (1990).

<sup>30</sup>S. Andersson, L. Wilzen, M. Persson, and J. Harris, *Phys. Rev. B* **40**, 8146 (1989).

<sup>31</sup>H. Schlichting and D. Menzel, *Surf. Sci.* **285**, 209 (1993).

<sup>32</sup>H. Schlichting and D. Menzel, *Rev. Sci. Instrum.* **64**, 2013 (1993).

<sup>33</sup>B. A. Chuikov, V. D. Osovskii, Yu. G. Ptushinskii, and V. G. Sukretnyi, *Surf. Sci.* **213**, 359 (1989).

<sup>34</sup>Yu. G. Ptushinskii, B. A. Chuikov, V. D. Osovskii, and V. G. Sukretnyi, *Fiz. Nizk. Temp.* **19**, 570 (1993) [*Low Temp. Phys.* **19**, 406 (1993)].

<sup>35</sup>W. Friess, H. Schlichting, and D. Menzel, *Phys. Rev. Lett.* **74**, 1147 (1995).

<sup>36</sup>H. Schlichting and D. Menzel, *Surf. Sci.* **272**, 27 (1992).

<sup>37</sup>D. A. King and M. G. Wells, *Surf. Sci.* **29**, 454 (1972).

<sup>38</sup>D. A. King and M. G. Wells, *Proc. R. Soc. London, Ser. A* **339**, 245 (1974).

<sup>39</sup>V. S. Bosov and B. A. Chuikov, *Ukr. Fiz. Zh.* **18**, 1568 (1973).

<sup>40</sup>Yu. G. Ptushinskii and B. A. Chuikov, *Surf. Sci.* **6**, 42 (1967).

<sup>41</sup>Yu. G. Ptushinskii and B. A. Chuikov, *Surf. Sci.* **7**, 90 (1967).

<sup>42</sup>R. Gomer and R. Wortman, *J. Chem. Phys.* **23**, 1741 (1955).

<sup>43</sup>R. Wortman, R. Gomer, and R. Lundy, *J. Chem. Phys.* **24**, 161 (1956).

<sup>44</sup>V. D. Osovskii, Yu. G. Ptushinskii, V. G. Sukretnyi, and B. A. Chuikov, *JETP Lett.* **67**, 959 (1998).

<sup>45</sup>P. W. Tamm and L. D. Schmidt, *J. Chem. Phys.* **54**, 4775 (1971).

<sup>46</sup>B. A. Chuikov, V. V. Dvurechenskikh, V. D. Osovskii, Yu. G. Ptushinskii, and V. G. Sukretnyi, *Surf. Sci.* **285**, 75 (1993).

<sup>47</sup>V. D. Osovskii, Yu. G. Ptushinskii, V. G. Sukretnyi, and B. A. Chuikov, *JETP Lett.* **60**, 586 (1994).

<sup>48</sup>V. V. Dvurechenskikh, V. D. Osovskii, Yu. G. Ptushinskii, V. G. Sukretnyi, and B. A. Chuikov, *Ukr. Fiz. Zh.* **37**, 716 (1992).

<sup>49</sup>B. A. Chuikov, V. D. Osovskii, Yu. G. Ptushinskii, and V. G. Sukretnyi, *Surf. Sci.* **448**, L201 (2000).

<sup>50</sup>A. Gross, S. Wilke, and M. Scheffler, *Phys. Rev. Lett.* **75**, 2718 (1995).

<sup>51</sup>M. Kay, G. R. Darling, S. Holloway, J. A. White, and D. M. Bird, *Chem. Phys. Lett.* **245**, 311 (1995).

<sup>52</sup>M. Beutl, M. Riedler, and K. D. Rendulic, *Chem. Phys. Lett.* **247**, 249 (1995).

<sup>53</sup>M. Beutl, M. Riedler, and K. D. Rendulic, *Chem. Phys. Lett.* **256**, 33 (1996).

<sup>54</sup>M. Beutl, J. Lesnik, and K. D. Rendulic, *Surf. Sci.* **429**, 71 (1999).

<sup>55</sup>B. A. Chuikov, V. D. Osovskii, Yu. G. Ptushinskii, and V. G. Sukretnyi, *Surf. Sci.* **473**, 143 (2001).

<sup>56</sup>C. T. Rettner, H. Stein, and E. K. Schweizer, *J. Chem. Phys.* **89**, 3337 (1988).

<sup>57</sup>V. D. Osovskii, Yu. G. Ptushinskii, V. G. Sukretnyi, and B. A. Chuikov, *Fiz. Nizk. Temp.* **27**, 1138 (2001) [*Low Temp. Phys.* **27**, 843 (2001)].

<sup>58</sup>V. D. Osovskii, Yu. G. Ptushinskii, V. G. Sukretnyi, and B. A. Chuikov, *Fiz. Nizk. Temp.* **23**, 779 (1997) [*Low Temp. Phys.* **23**, 587 (1997)].

<sup>59</sup>N. V. Petrova, I. N. Yakovkin, and Yu. G. Ptushinskii, *Surf. Sci.* **497**, 349 (2002).

- <sup>60</sup>L. Wilzen, S. Andersson, and J. Harris, *Surf. Sci.* **205**, 387 (1988).
- <sup>61</sup>I. L. Silvera, *Rev. Mod. Phys.* **52**, 393 (1980).
- <sup>62</sup>E. A. Moelwyn-Hughes, *Physical Chemistry*, 2nd ed., Pergamon Press, Oxford (1961), Izd-vo Inostr. Lit., Moscow (1982).
- <sup>63</sup>V. V. Gonchar, O. V. Kanash, A. G. Naumovets, and A. G. Fedorus, *JETP Lett.* **28**, 330 (1978).
- <sup>64</sup>V. V. Gonchar, O. V. Kanash, and A. G. Fedorus, *JETP Lett.* **38**, 189 (1983).
- <sup>65</sup>V. V. Gonchar, Yu. M. Kagan, O. V. Kanash, A. G. Naumovets, and A. G. Fedorus, *Zh. Éksp. Teor. Fiz.* **84**, 249 (1983) [*Sov. Phys. JETP* **57**, 142 (1983)].
- <sup>66</sup>V. V. Gonchar, O. V. Kanash, I. A. Kotlyarova, A. G. Fedorus, and A. A. Fedosenko, *Zh. Éksp. Teor. Fiz.* **95**, 1773 (1989) [*Sov. Phys. JETP* **68**, 1023 (1989)].
- <sup>67</sup>A. G. Fedorus, V. V. Gonchar, O. V. Kanash, E. V. Klimenko, A. G. Naumovets, and I. N. Zasimovich, *Surf. Sci.* **251/252**, 846 (1991).
- <sup>68</sup>A. G. Fedorus, E. V. Klimenko, A. G. Naumovets, E. M. Zasimovich, and I. N. Zasimovich, *Nucl. Instrum. Methods Phys. Res. B* **10**, 207 (1995).
- <sup>69</sup>O. M. Braun and É. A. Pashitskiĭ, *Poverkhnost'. Fiz. Khim. Mekh.*, No. 7, 49 (1984).
- <sup>70</sup>R. Di Foggio and R. Gomer, *Phys. Rev. B* **25**, 3490 (1982).
- <sup>71</sup>V. G. Peschanskiĭ and M. Ya. Azbel', *Zh. Éksp. Teor. Fiz.* **55**, 1980 (1968) [*Sov. Phys. JETP* **28**, 1045 (1969)].
- <sup>72</sup>O. A. Panchenko and P. P. Lutsishin, *Zh. Éksp. Teor. Fiz.* **57**, 1555 (1969) [*Sov. Phys. JETP* **30**, 841 (1970)].
- <sup>73</sup>O. A. Panchenko, P. P. Lutsishin, Yu. G. Ptushinskii, and V. V. Shishkov, *Surf. Sci.* **34**, 187 (1973).
- <sup>74</sup>A. F. Andreev, *Usp. Fiz. Nauk* **105**, 113 (1971) [*Sov. Phys. Usp.* **14**, 609 (1972)].
- <sup>75</sup>O. A. Panchenko, A. A. Kharlamov, and Yu. G. Ptushinskiĭ, *Zh. Éksp. Teor. Fiz.* **67**, 780 (1974) [*Sov. Phys. JETP* **40**, 386 (1975)].
- <sup>76</sup>A. A. Kharlamov, O. A. Panchenko, and Yu. G. Ptushinskii, *Solid State Commun.* **15**, 1793 (1974).
- <sup>77</sup>P. P. Lutsishin, O. A. Panchenko, and S. V. Sologub, *Poverkhnost'. Fiz. Khim. Mekh.*, No. 8, 22 (1987).
- <sup>78</sup>P. P. Lutsishin, O. A. Panchenko, and V. E. Shpagin, *Surf. Sci.* **278**, 218 (1992).
- <sup>79</sup>P. P. Lutsishin, O. A. Panchenko, and S. V. Sologub, *Poverkhnost'. Fiz. Khim. Mekh.*, No. 11, 69 (2001).
- <sup>80</sup>H. F. Berger, M. Leisch, A. Winkler, and K. D. Rendulic, *Chem. Phys. Lett.* **175**, 425 (1990).
- <sup>81</sup>H. F. Berger and K. D. Rendulic, *Surf. Sci.* **253**, 325 (1991).
- <sup>82</sup>B. E. Hayden and C. L. A. Lamont, *Chem. Phys. Lett.* **160**, 331 (1989).
- <sup>83</sup>C. T. Rettner, M. A. Michelsen, and D. J. Auerbach, *J. Chem. Phys.* **102**, 4625 (1995).
- <sup>84</sup>M. Gruyters and K. Jacobi, *Chem. Phys. Lett.* **225**, 309 (1994).
- <sup>85</sup>K. Svensson and S. Andersson, *Surf. Sci.* **392**, L40 (1997).
- <sup>86</sup>E. Ilicsa, *Phys. Rev. Lett.* **66**, 667 (1991).
- <sup>87</sup>S. Andersson and J. Harris, *Phys. Rev. B* **27**, 9 (1983).
- <sup>88</sup>M. Beutl, E. Lunden, C. Konvicka, P. Varga, and K. D. Rendulic, *Surf. Sci.* **447**, 245 (2000).
- <sup>89</sup>M. Persson and S. Andersson, *Surf. Rev. Lett.* **1**, 187 (1994).
- <sup>90</sup>S. Andersson and M. Persson, *Phys. Rev. Lett.* **70**, 202 (1993).
- <sup>91</sup>S. Andersson and M. Persson, *Phys. Rev. B* **48**, 5685 (1993).
- <sup>92</sup>S. Andersson, M. Persson, and J. Harris, *Surf. Sci.* **360**, L499 (1996).
- <sup>93</sup>K. Svensson, L. Bengtsson, J. Bellman, M. Hassel, M. Persson, and S. Andersson, *Phys. Rev. Lett.* **83**, 124 (1999).
- <sup>94</sup>L. Bengtsson, K. Svensson, M. Hassel, J. Bellman, M. Persson, and S. Andersson, *Phys. Rev. B* **61**, 16921 (2000).
- <sup>95</sup>J. N. Chubb, L. Gowland, and I. E. Pollard, *J. Phys. D* **1**, 361 (1968).
- <sup>96</sup>C. Benvenuti, R. S. Calder, and G. Passardi, *J. Vac. Sci. Technol.* **13**, 1172 (1976).
- <sup>97</sup>J. Cui, S. C. Fain, Jr, and W. Liu, *J. Vac. Sci. Technol. A* **7**, 1850 (1989).
- <sup>98</sup>P. M. Ferm, S. M. Kurtz, and K. A. Pearlstine, *Phys. Rev. Lett.* **58**, 2602 (1987).
- <sup>99</sup>K. A. Pearlstine and G. M. McClelland, *Surf. Sci.* **134**, 389 (1983).
- <sup>100</sup>M. Hassel, K. Svensson, M. Persson, and S. Andersson, *Phys. Rev. Lett.* **80**, 2481 (1998).
- <sup>101</sup>M. Hassel, K. Svensson, J. Bellman, S. Andersson, and M. Persson, *Phys. Rev. B* **65**, 205402 (2002).
- <sup>102</sup>K. Svensson and S. Andersson, *Phys. Rev. Lett.* **78**, 2016 (1997).
- <sup>103</sup>W. Rühl, *Z. Phys.* **176**, 409 (1963).
- <sup>104</sup>G. Chottiner and R. E. Glover, *J. Vac. Sci. Technol. A* **15**, 429 (1978).
- <sup>105</sup>C. Leung and R. Gomer, *Surf. Sci.* **59**, 638 (1976).
- <sup>106</sup>Yu. G. Ptushinskiĭ and B. A. Chuikov, *Fiz. Tverd. Tela (Leningrad)* **10**, 722 (1968) [*Sov. Phys. Solid State* **10**, 565 (1968)].
- <sup>107</sup>C. Wang and R. Gomer, *Surf. Sci.* **74**, 389 (1978).
- <sup>108</sup>H. Michel, R. Opila, and R. Gomer, *Surf. Sci.* **105**, 48 (1981).
- <sup>109</sup>R. Opila and R. Gomer, *Surf. Sci.* **105**, 41 (1981).
- <sup>110</sup>A. N. Artsyukovich and V. A. Ukrainsev, *Surf. Sci.* **347**, 303 (1996).
- <sup>111</sup>V. D. Osovskii, Yu. G. Ptushinskii, V. G. Sukretnyi, B. A. Chuikov, V. K. Medvedev, and Yu. Suchorski, *Surf. Sci.* **377-379**, 664 (1997).
- <sup>112</sup>B. G. Briner, M. Doering, H.-P. Rust, and A. M. Bradshaw, *Phys. Rev. Lett.* **78**, 1516 (1997).
- <sup>113</sup>V. V. Zhukov, V. D. Osovskii, Yu. G. Ptushinskiĭ, V. G. Sukretnyi, and B. A. Chuikov, *Ukr. Fiz. Zh.* **31**, 1374 (1986).
- <sup>114</sup>V. V. Zhukov, V. D. Osovskii, Yu. G. Ptushinskiĭ, V. G. Sukretnyi, and B. A. Chuikov, *Izv. AN SSSR Ser. Fiz.* **52**, 1462 (1988).
- <sup>115</sup>C. T. Rettner, E. K. Schweizer, and H. Stein, *J. Chem. Phys.* **93**, 1442 (1990).
- <sup>116</sup>H. P. Steinruck and R. J. Madix, *Surf. Sci.* **185**, 36 (1987).
- <sup>117</sup>C. Wang and R. Gomer, *Surf. Sci.* **84**, 329 (1979).
- <sup>118</sup>D. Schmeisser and K. Jacobi, *Surf. Sci.* **108**, 421 (1981).
- <sup>119</sup>Ya-po Hsu, K. Jacobi, and H. H. Rottermund, *Surf. Sci.* **117**, 581 (1981).
- <sup>120</sup>A. C. Lunz, J. Grimblot, and D. E. Fowler, *Phys. Rev. B* **39**, 12903 (1989).
- <sup>121</sup>W. Ranke, *Surf. Sci.* **209**, 57 (1989).
- <sup>122</sup>A. Eichler and J. Hafner, *Phys. Rev. Lett.* **79**, 4481 (1997).
- <sup>123</sup>J. Beckerle, O. Yang, A. Jonson, and S. Ceyer, *Surf. Sci.* **195**, 77 (1988).
- <sup>124</sup>R. Franchy, T. U. Bartke, and P. Gassmann, *Surf. Sci.* **366**, 60 (1996).
- <sup>125</sup>K. B. K. Tang, J. Villette, D. Teillet-Billy, J. P. Gauyacq, and R. E. Palmer, *Surf. Sci.* **368**, 43 (1996).
- <sup>126</sup>S. Lacombe, F. Cemič, P. He, H. Dietrich, P. Geng, and K. Jacobi, *Surf. Sci.* **368**, 38 (1996).
- <sup>127</sup>M. Shayegan, J. M. Cavallo, R. E. Glover, III, and R. L. Park, *Phys. Rev. Lett.* **53**, 1578 (1984).
- <sup>128</sup>G. Bader, G. Petruzzo, L. G. Caron, and L. Sanche, *Phys. Rev. B* **30**, 78 (1984).
- <sup>129</sup>W. Wurth, J. Stöhr, P. Feulner, K. R. Bauchspiess, Y. Baba, E. Hudel, G. Rocker, and D. Menzel, *Phys. Rev. Lett.* **65**, 2426 (1990).
- <sup>130</sup>P. P. Lutsishin, T. N. Nakhodkin, O. A. Panchenko, and Yu. G. Ptushinskiĭ, *JETP Lett.* **31**, 563 (1980).
- <sup>131</sup>V. I. Vatamanyuk, D. A. Gorodetskiĭ, A. G. Kundzich, P. P. Lutsishin, Yu. P. Mel'nik, O. A. Panchenko, V. A. Usenko, and A. A. Yas'ko, *Poverkhnost'. Fiz. Khim. Mekh.*, No. 1, 18 (1990).
- <sup>132</sup>C. Leung, M. Vass, and R. Gomer, *J. Vac. Sci. Technol.* **13**, 286 (1976).
- <sup>133</sup>P. R. Norton, R. L. Tapping, and J. W. Goodale, *Surf. Sci.* **72**, 33 (1978).
- <sup>134</sup>J. E. Demuth, D. Schmeisser, and Ph. Avouris, *Phys. Rev. Lett.* **47**, 1166 (1981).
- <sup>135</sup>M. Shayegan, E. D. Williams, R. E. Glover, III, and R. L. Park, *Surf. Sci.* **154**, L239 (1985).
- <sup>136</sup>J. Yoshinobu and M. Kawai, *Surf. Sci.* **363**, 105 (1996).
- <sup>137</sup>M. Kawai and J. Yoshinobu, *Surf. Sci.* **368**, 239 (1996).
- <sup>138</sup>P. Sautet, M. K. Rose, J. C. Dumphy, S. Behler, and M. Salmeron, *Surf. Sci.* **453**, 25 (2000).
- <sup>139</sup>M. J. Grunze, J. Fuhler, M. Neumann, C. R. Brundle, D. J. Auerbach, and J. Behm, *Surf. Sci.* **139**, 109 (1984).
- <sup>140</sup>D. Schmeisser, K. Jacobi, and D. M. Kolb, *Vacuum* **31**, 439 (1981).
- <sup>141</sup>F. Bartolucci and R. Franchy, *Surf. Sci.* **368**, 27 (1996).
- <sup>142</sup>K. Jacobi, M. Bertolo, P. Geng, W. Hansen, and C. Astaldi, *Chem. Phys. Lett.* **173**, 97 (1990).

Translated by Steve Torstveit